Transition Metal Catalysis in Living Cells

Progress, Challenges, and Novel Supramolecular Solutions

James, C.C.; de Bruin, B.; Reek, J.N.H.

DOI
10.1002/ange.202306645
10.1002/anie.202306645

Publication date
2023

Document Version
Final published version

Published in
Angewandte Chemie

Zitierweise: *Angew. Chem. Int. Ed.* **2023**, *62*, e202306645
doi.org/10.1002/anie.202306645

Catalysis

Transition Metal Catalysis in Living Cells: Progress, Challenges, and Novel Supramolecular Solutions

*Catriona C. James, Bas de Bruin, and Joost N. H. Reek**

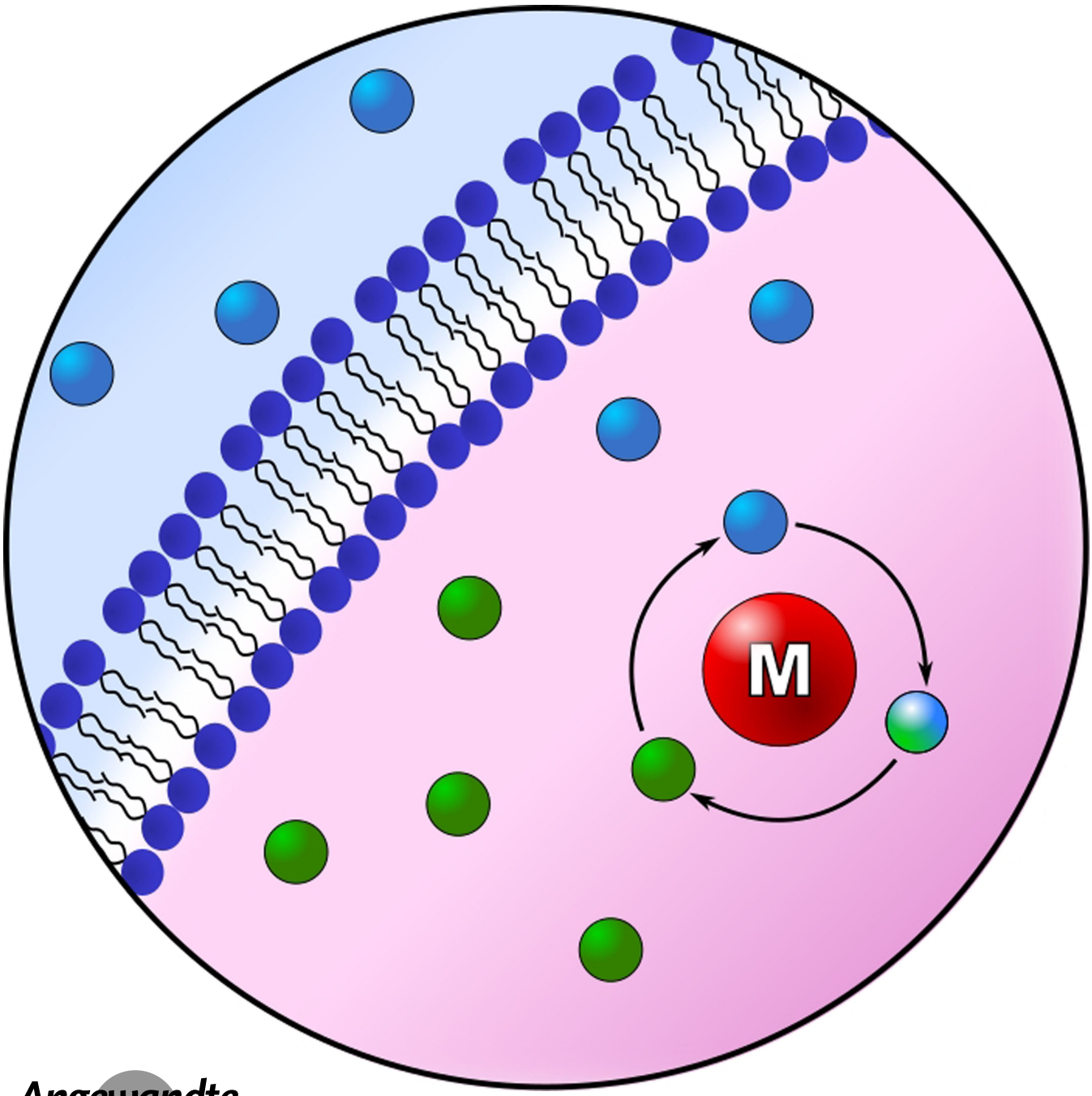

Angewandte Chemie

Abstract: The importance of transition metal catalysis is exemplified by its wide range of applications, for example in the synthesis of chemicals, natural products, and pharmaceuticals. However, one relatively new application is for carrying out new-to-nature reactions inside living cells. The complex environment of a living cell is not welcoming to transition metal catalysts, as a diverse range of biological components have the potential to inhibit or deactivate the catalyst. Here we review the current progress in the field of transition metal catalysis, and evaluation of catalysis efficiency in living cells and under biological (relevant) conditions. Catalyst poisoning is a ubiquitous problem in this field, and we propose that future research into the development of physical and kinetic protection strategies may provide a route to improve the reactivity of catalysts in cells.

1. Introduction

Catalysis is an invaluable tool for many different areas of chemistry. Transition metal catalysts provide a facile route to achieve otherwise difficult transformations, such as carbon-carbon bond forming reactions. As a result, transition metal catalysis plays a pivotal role in a vast range of applications, for example the synthesis of natural products and bioactive compounds, and the development of pharmaceuticals.[1] Although chemists have harnessed the powerful reactivity of transition metals to gain access to these useful compounds, nature is able to selectively and efficiently synthesise complex molecules using a different set of tools. In cells catalysis is naturally carried out by enzymes: simple amino acid building blocks are joined together to generate intricate 3D structures that are responsible for mediating the production of a huge range of compounds that are necessary for the functioning of the cell. While enzyme catalysis is celebrated for achieving levels of selectivity, which chemists are often unable to match with synthetic metal catalysts, this selectivity comes with a price. The substrate scope for a particular enzyme can be very small, and if the desired target compound for a reaction is not naturally produced in the cell, there may not be a naturally occurring enzyme available that is able to catalyse the desired reaction.[2] Therefore an exogenous catalyst to carry out reactions in cells that are new to nature is an interesting area to explore.

Catalytically controlling reactions in living cells has important applications for biomolecular labelling and imaging, as well as for pharmaceuticals. Catalytic activation of prodrugs provides the opportunity for localised drug activation, which in the context of cancer treatment could help to decrease system-wide toxicity and reduce the fairly severe side effects that are typically associated with traditional chemotherapy. Therefore, achieving selective, efficient, bioorthogonal catalysis for new to nature reactions is an important goal. This need has brought about the birth of a relatively new field, where transition metal catalysts are applied in living cells. Using a synthetic transition metal catalyst, instead of endogenous or modified enzymes, provides the means to increase the reaction and substrate scopes to obtain non-natural reactivity. Another advantage of transition metals is that it is relatively easy to tune the metal centre to achieve the desired reactivity, by modifying the ligands surrounding the metal centre.

Over the last 20 years there have been many examples of transition metal catalysis either inside or in the presence of living cells.[3] However, this field is still in its infancy. Poor catalytic activity is ubiquitous, and low yields, very high catalyst loadings, and low turnover numbers (TON), if these numbers can be determined at all, are generally encountered. This is in stark contrast to the high yields and efficiencies that are observed for applications outside of the biological setting. Therefore, new strategies are required to improve the reactivity of transition metal catalysts in biological settings. This review highlights the progress already achieved in this field, and proposes which new areas of research may solve some of the problems currently faced.

2. Transition Metal Catalysis in Biological Systems

The root of the challenges faced in the field of catalysis in living cells is that the conditions within a cell are very hostile towards transition metals and the reactions that they catalyse. The first hurdle to overcome is entry of the reaction components into the inside of the cell. Prokaryotic cells, such as bacteria, are enclosed by a cell wall, which is permeable to most compounds. Beyond the cell wall is the periplasm, which is separated from the interior of the cell (the cytoplasm) by a cell membrane. In contrast, eukaryotic cells, such as mammalian cells, are enclosed only by a cell membrane. The cell membrane is comprised of an amphiphilic phospholipid bilayer, the structure of which is shown in Figure 1. The head of the phospholipid is a hydrophilic phosphate group, which points outwards into the extracellular space, and inwards towards the cytosol; meanwhile hydrophobic lipid tails comprise the interior of the cell membrane. This means that while small neutral compounds can easily diffuse through the cell membrane, large hydrophilic or charged species are often impermeable and are unable to pass through the membrane.[4] Once the reaction components have crossed the cell membrane to enter the cell, the next challenge is the compatibility of the reaction

[*] Dr. C. C. James, Prof. Dr. B. de Bruin, Prof. Dr. J. N. H. Reek
van't Hoff Institute for Molecular Sciences,
University of Amsterdam
Science Park 904, 1098 XH Amsterdam (The Netherlands)
E-mail: j.n.h.reek@uva.nl

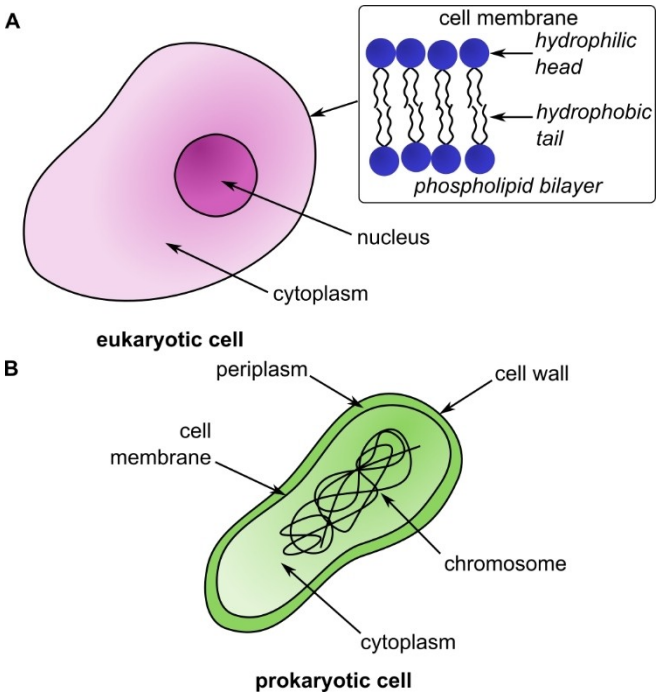

Figure 1. Basic structures of A) eukaryotic and B) prokaryotic cells, and the phospholipid bilayer cell membrane.

itself with the cell. Cells have an aqueous aerobic environment, and many reactions catalysed by metals are not tolerant to water and/or oxygen. Nevertheless, even after selecting a water and oxygen-tolerant reaction, the specific conditions required to sustain most biological systems still have to be adhered to. The temperature of human cells is 37 °C, the pH in living systems is typically around 7, and high salt concentrations are typically present. In addition, there are high quantities of nucleophiles and thiols, the most notable of which is glutathione (GSH), which is found in 1–10 mM, and commonly poisons transition metal catalysts.[5] Finally, whereas in a normal synthetic reaction there would only be substrate present, there is a huge variety of other biomolecules present in a cell, which in principle could compete with your desired substrate, or also inhibit the catalysis.

Despite these challenges, it is still possible to successfully carry out transition metal catalysis inside living cells. There are three general strategies used for transition metal catalysis in biological systems: 1) a discrete, molecular catalyst is deployed; 2) large, composite structures, such as nanoparticles, nanozymes, or other supramolecular structures; and 3) artificial metalloenzymes, where molecular catalysts are docked inside a protein scaffold. A diverse range of catalysts of all three of these types have been used under biological conditions (where experiments are carried out in the lab in the presence of biological additives or in cell culture media), in living cells (*in vitro*; where catalysis is carried out inside cells that have been cultured on a plate), and even in whole organisms (*in vivo*; where the reaction components are injected into a living animal such as a mouse or zebrafish embryo). Additionally, a wide range of different types of reactions have been employed for catalysis in living cells. Many initial studies utilise relatively simple transformations, such as redox reactions, transfer hydrogenations,

Catriona James obtained her Master's in general chemistry from the University of Glasgow. She then obtained her Ph.D. in in vivo transition metal catalysis at the University of Amsterdam under the supervision of Prof. B. de Bruin and Prof. J. N. H. Reek. Her research interests lie at the interface between biology and chemistry, with a focus on homogeneous catalysis and supramocular chemistry.

Bas de Bruin obtained his Ph.D. at the university of Nijmegen under supervision of Anton Gal. He did his postdoc in the group of Karl Wieghardt at the MPI für Bioanorganische Chemie (Mülheim a/d Ruhr, Germany, 1999–2000). After his postdoc he returned to the University of Nijmegen as an assistant professor. November 2005 he moved to the University of Amsterdam (UvA), where he was promoted to full professor in 2013. His research focuses at the development of new tools in homogeneous catalysis, using metallo-radicals and unconventional ligands, specifically aiming at the development of new catalytic reactions for various applications.

Joost Reek obtained his Ph.D. at the University of Nijmegen under supervision of Prof. R. J. M. Nolte in the area of supramolecular chemistry. After a postdoc with Prof. Crossley in Sydney, he moved to the University of Amsterdam in 1998, where he was promoted to full professor in 2006, and faculty professor in 2017. His research interests include homogeneous catalysis and supramolecular chemistry, and he is exploring new research on the border of these research topics. In addition, he has an interest in develping solar to fuel devices based on molecular components, with a focus on the catalytic processes involved. More recently he has been exploring supramolecular chemistry and catalysis in living systems to extend some of the concepts to other areas of application.

or deprotection reactions. However, more complex, bond-making systems have also been developed, including both intra- and intermolecular cyclisation reactions, and even cross-coupling reactions. Here, the efficiency of different catalysts for each type of reaction will be discussed, if this information is available. The analysis and quantification of catalysis in cells is challenging, as many of the typical techniques used for monitoring a catalytic reaction (for example, NMR spectroscopy or GC analysis) are unable to be applied to the cellular setting. Therefore, one of the most straightforward ways to determine if a reaction is successful is to design a system where the product results in the "switch-on" of a easily monitored property, such as fluorescence or cytotoxicity. For this reason, almost all reactions in living cells involve the synthesis or activation of a fluorescent dye or cytotoxic drug. The structures of the most commonly used dyes and drugs are illustrated in Figure 2. However, although this provides a handle for a simple confirmation if the reaction worked at all, it is often challenging to quantify yields or TONs of reactions. This is in part because often the uptake efficiencies of all the components of the reaction are unknown, so the actual concentration of substrate and the real catalyst loading inside the cell is not clearly defined, so often it is only possible to obtain qualitative data about the reaction efficiency. It should therefore be noted that while we (and others) use catalysis, it is often unknown what turnover was reached after the reaction, and therefore whether or not the reaction was catalytic or stoichiometric in nature in the cells. The following sections will discuss the efficiencies of reactions that have been carried out inside the cytoplasm of cells (rather than extracellularly, on cells, or in the periplasm) by molecular catalysts, and analyse what aspects of these reactions should be improved.

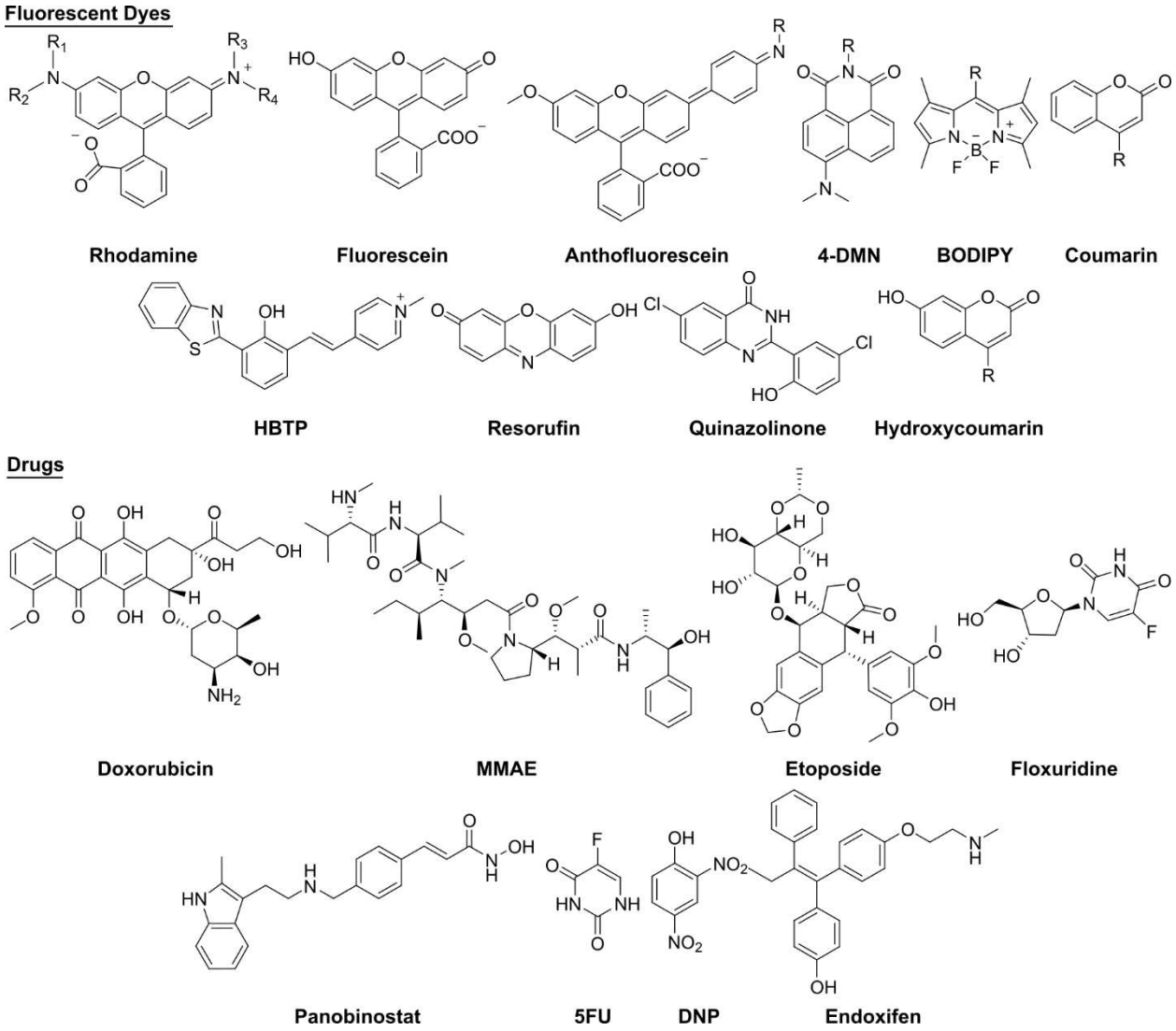

Figure 2. Structures of drugs and fluorescent dyes that are commonly used as the product of a transition metal catalysed reaction inside living cells.

2.1. Oxidation and Reduction Reactions

Various types of redox reactions have been used to exploit chemical conversions in cells aiming for different goals; for example, influencing the cellular redox balance, and chemical and photoreductions to generate fluorophores and drugs. The maintenance of the cellular redox balance is vital for a range of processes, including cellular metabolism, cell death, cell differentiation and development, immune responses, and circadian rhythm. Cellular redox homeostasis is the process by which oxidising and reducing reactions within the cell are kept in balance, and is maintained by several reducing agents, such as glutathione, thioredoxin, and reduced nicotinamide adenine dinucleotide (NADH).[6] Therefore, altering the intracellular concentrations of these compounds can have serious consequences for the viability of the cells. Sadler et al. used this alteration to their advantage, by using Ru^{II} piano-stool complexes to catalyse the oxidation of glutathione to its dimer, GSSG (Figure 3a). This reactivity was monitored in A549 human lung cancer cells via an increase in reactive oxygen species (ROS) and the resultant decrease in cell survival.[7] Since glutathione is

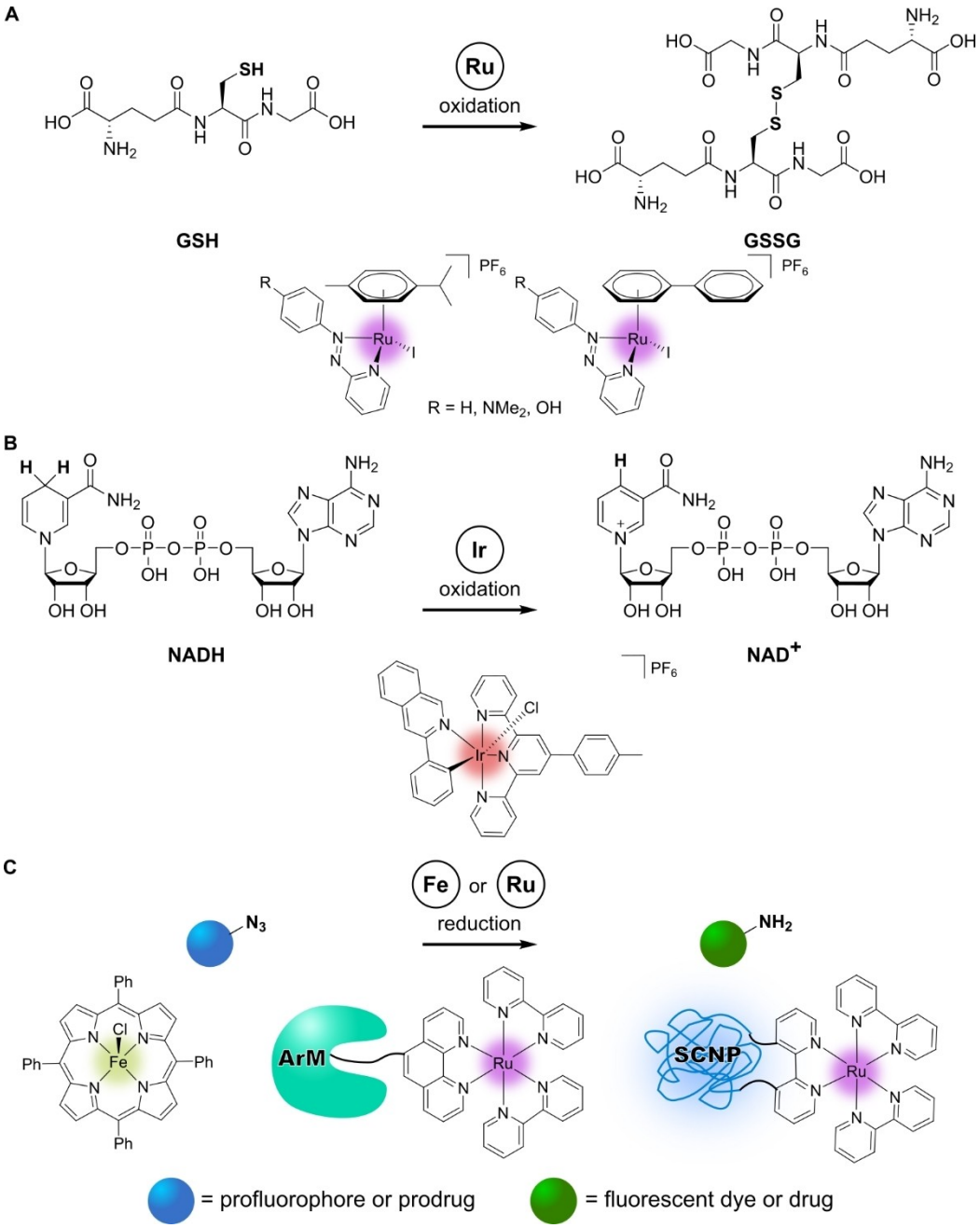

Figure 3. Overview of the oxidation and reduction reactions carried out in cells. (a) Ruthenium catalysed glutathione oxidation (Ref. [7]). (b) Iridium catalysed NADH oxidation (Ref. [9]). (c) Iron and ruthenium catalysed azide reduction (Refs. [11–16]).

the primary antioxidant in cells, a decrease of the glutathione levels induces this build-up of ROS (Figure 4), ultimately leading to cell death.[8]

Recently, the same group developed a cyclometallated Ir^{III} photoredox catalyst, which catalyses both the photooxidation of NADH to NAD^+ and the concurrent photoreduction of cytochrome *c* (cyt *c*) (Figure 3b). The catalytic cycle is depicted in Figure 5a. After excitation with blue light, the complex extracts an electron from NADH to generate the radical cation, which is readily deprotonated to form the neutral carbon-centred radical, NAD•. Under regular oxygen levels (20 % O_2), molecular oxygen re-oxidises the iridium complex while generating superoxide radicals, which extracts an electron from NAD• and consumes two protons from the surrounding medium, to generate NAD^+ and peroxide. However, in hypoxic cells (1 % O_2), such as A549 lung cancer cells, oxidised cytochrome c (cyt c_{ox}) can replace the role of the superoxide radicals, and is reduced by both the iridium(II) intermediate and the NAD• radical. This cellular catalysis resulted in a significant decrease in NADH and disrupted the mitochondrial electron transport chain (ETC), as evidenced by a decrease in the mitochondrial membrane potential.[9] The mitochondrial ETC is responsible for generating energy in the form of adenosine triphosphate (ATP) during cellular respiration, and the first step of this chain is oxidation of NADH (Figure 5b). Therefore, decreasing the amount of NADH available inhibits the generation of ATP, which results in cell death in the form of apoptosis and necrosis.[10] Lower toxicity towards normal cells in the dark compared to cancer cells in the light was observed.[9]

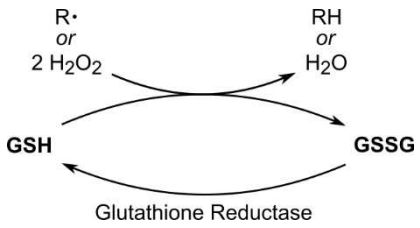

Figure 4. GSH-mediated regulation of ROS levels in cells.

The only iron complex that has been used in living cells so far is an Fe^{III} porphyrin complex ([Fe(TPP)Cl]) by Meggers et al., to catalytically reduce aryl azides, using a cellular thiol, cysteine, as reducing agent (Figure 3c). The generation of bisazide-protected rhodamine 110 appeared to be successful in HeLa cells, with 10 mol % of the catalyst resulting in a 28-fold increase in fluorescence in just 10 minutes. However, when the same reaction was applied in nematodes and zebrafish, a fluorescence signal increase was observed in the absence of catalyst, with the addition of catalyst having no effect on the signal, demonstrating that the bisazide was able to be metabolically reduced without the need for a metal catalyst.[11]

In an alternative strategy to achieve azide reduction, Winssinger et al. have developed ruthenium^{II} artificial metalloenzymes (ArMs) to photocatalytically reduce azides under biological conditions. Both the catalyst, $[Ru(bpy)_2(phen)]$, and azide-protected rhodamine were covalently attached to biotin, and both were docked inside an oligomeric receptor, in order to bring the catalyst and substrate in close proximity (Figure 6). The selected target protein, acetyl CoA carboxylase (ACC), is a biotin-binding multicomponent protein found in *P. aeruginosa*, a pathogenic bacteria that does not contain streptavidin. Although the reaction requires stoichiometric amounts of sodium ascor-

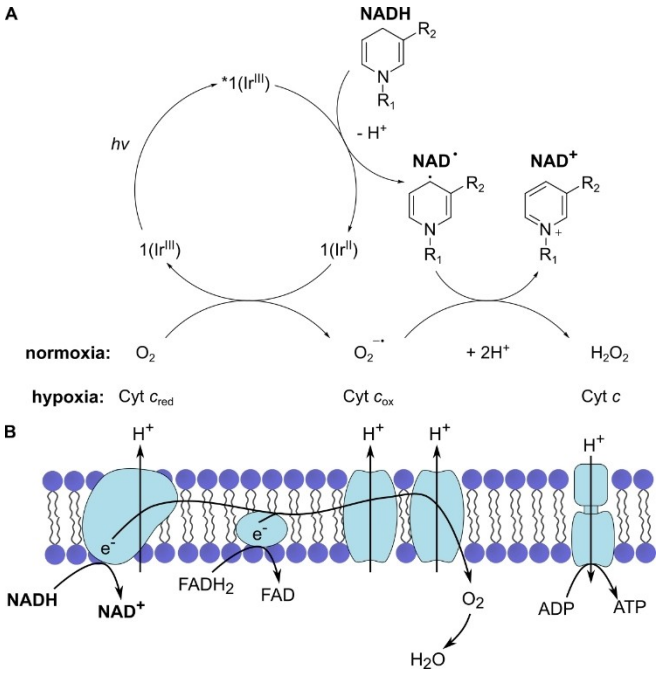

Figure 5. (a) Catalytic cycle for the iridium photocatalysed oxidation of NADH to NAD^+ via a neutral carbon radical NAD• intermediate. Under normoxic conditions the iridium complex is re-oxidised by molecular oxygen; under hypoxic conditions the iridium complex is re-oxidised by cyt *c*. (b) The electron transport chain that takes place in the mitochondrial membrane, which relies upon NADH to generate energy in the form of ATP.

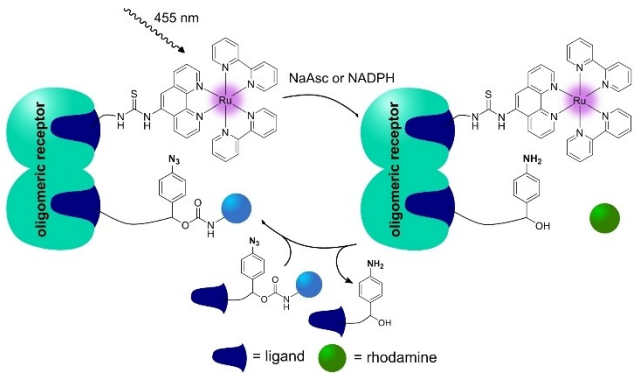

Figure 6. Schematic representation of both the artificial metalloenzyme with ruthenium photocatalyst and azide-protected rhodamine docked inside the protein. Following irradiation with blue light the ruthenium catalyst reduces the azide to an amine, which then cleaves and activates the rhodamine.

bate to act as a reducing agent under biological conditions in the lab, when the reaction was carried out *in vitro*, it appeared that the cellular environment is sufficiently reducing to allow the reaction to proceed in the absence of sodium ascorbate. Presumably NADH acts as the reducing agent, leading to an 8-fold increase in fluorescence after irradiation with blue light. Following the success in bacteria, the system was also applied in MCF-7 cancer cells.[12] The system was expanded to different proteins and docking moieties, to generate a quinazolinone-based precipitating dye (QPD). Intracellular reactivity was achieved by linking the complex to raloxifene, an oestrogen receptor-agonist, which binds to the oestrogen receptor in MCF-7 cells. Activation of the dye localised in the nucleus was observed.[13]

The same photocatalytic ruthenium artificial metalloenzyme model was modified to make use of azide reduction for the labelling of micro RNA (miRNA). For this goal, the catalyst and the dye were bound to peptide nucleic acid (PNA) strands, an artificial polymer that is similar to DNA or RNA, where the backbone is comprised of *N*-(2-aminoethyl)-glycine units linked by peptide bonds. The PNA binds to base-matched miRNA, bringing the dye and the catalyst together, and reduction of an aryl azide within the dye linker releases a rhodamine-based dye (Figure 7). This reaction was carried out in BT474 human breast cancer cells that display a high expression of the corresponding miRNA when either sodium ascorbate or NADH were used as the reducing agent. Some fluorescence was also observed in the cells without the addition of an external reducing agent, which indicates that endogenous levels of NADH are suitable for the reaction.[14] Finally, the reaction was also carried out in zebrafish embryos, which is the first example of in vivo miRNA detection.[15]

A recent example of in vitro photocatalytic azide reduction was used both concurrently and in tandem with an endogenous enzyme. A $[Ru(bpy)_3]$ catalyst incorporated within a single chain nanoparticle (SCNP) was able to photocatalytically activate azide-protected rhodamine 110 in the cytosol of HeLa cells (Figure 8). The Ru-SCNP was bound to the *β*-Gal, and the Ru-SCNP-*β*-Gal complex was used to carry out tandem reactions to synthesise hydroxycoumarin. Photocatalytic azide reduction by the Ru-SCNP produced a galactose-protected intermediate, which then could be converted into hydroxycoumarin by the *β*-Gal. However, this was unsuccessful in live HeLa cells, possibly due to substrate cell permeability, but it was found to work well in *E. coli*.[16]

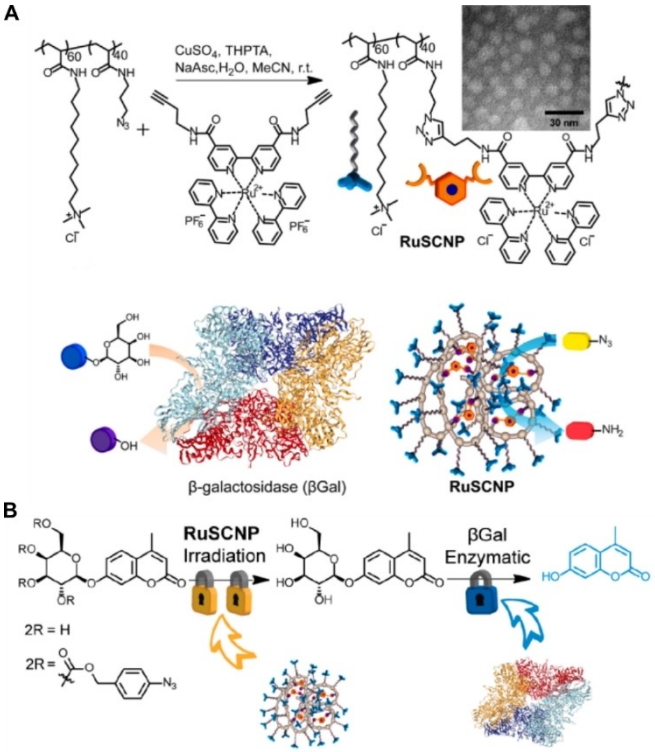

Figure 8. (a) Structure and synthesis of the Ru-SCNP. The water soluble polymer is intramolecularly cross-linked to the ruthenium photocatalyst using a CuAAC reaction. (b) Ru-SCNP-*β*-Gal tandem reaction that generates hydroxycoumarin. Reproduced with permission.[16] 2020, ACS Publications.

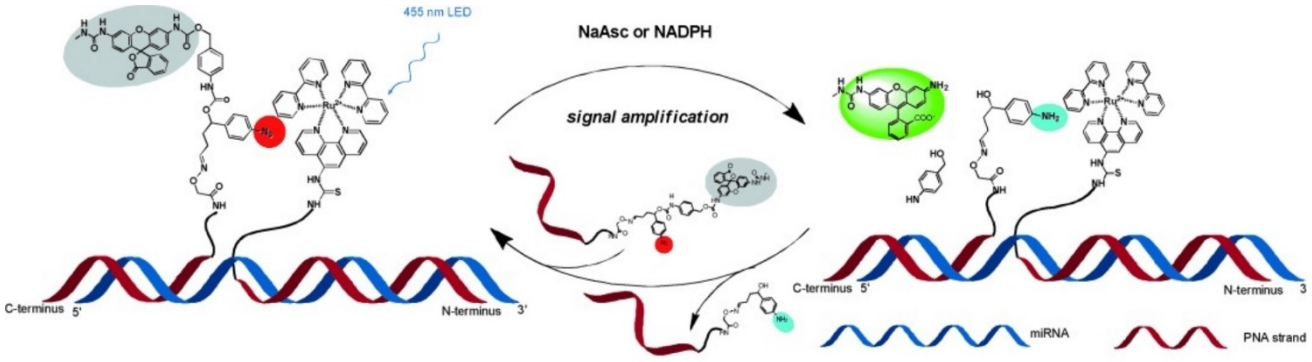

Figure 7. Schematic representation of the miRNA-templated azide reduction. The ruthenium photocatalyst and the azide-protected rhodamine are bound to PNA, which binds to the miRNA. The ruthenium photocatalyst reduces the azide to an amine following irradiation with blue light, which releases the activated rhodamine. Reproduced with permission.[14] 2013, Wiley Publishing.

2.2. Transfer Hydrogenation

Transfer hydrogenation is a frequently used chemical transformation performed inside living cells, and is commonly catalysed by iridium piano-stool complexes (Figure 9a). These types of Ir^{III} complexes have been used for the hydrogenation of aldehydes or ketones to alcohols, using NADH as the hydride source. Although this reaction is water and air tolerant, the efficacy of the reaction is very much dependent on the presence of various biomolecules. Using a BODIPY-based probe, iridium complexes were used to reduce an aldehyde (BODIPY-CHO) to a fluorescent alcohol (BODIPY-OH), with NADH used as the hydride source. The reaction was carried out in the cytoplasm of NIH-3T3 mouse embryo fibroblast cells. Even though the probe was incubated with a huge catalyst loading of 66 mol %, only a 1.6-fold increase in fluorescence was observed, whereas when the BODIPY-OH probe was administered alone the fluorescence change was 2.2 fold, indicating that full conversion to the product was not achieved by the catalyst.[17]

Transfer hydrogenation from NADH to oxygen in order to induce cell death, has also been demonstrated in cancer cells (Figure 9b). This reactivity was first reported for cyclometalated iridium complexes. After incubation in A2780 human ovarian cancer cells, a decrease in cell proliferation was observed. This was attributed to catalytic hydrogen transfer from NADH to oxygen, as a large increase in ROS and peroxides was observed. Not surprisingly, the presence of glutathione was found to deactivate the complexes.[18] A series of similar Ir^{III} complexes were then used as a co-medicine in combination with cisplatin and carboplatin to enhance cancer cell death. When the metal complexes are incubated in cancer cells, the iridium catalyst converts NADH to NAD^+, generating an iridium-hydride complex. The change in this NADH/NAD^+ ratio chemosensitises the cancer cells to the platinum drugs, which increases their efficacy. The iridium-hydride complex can

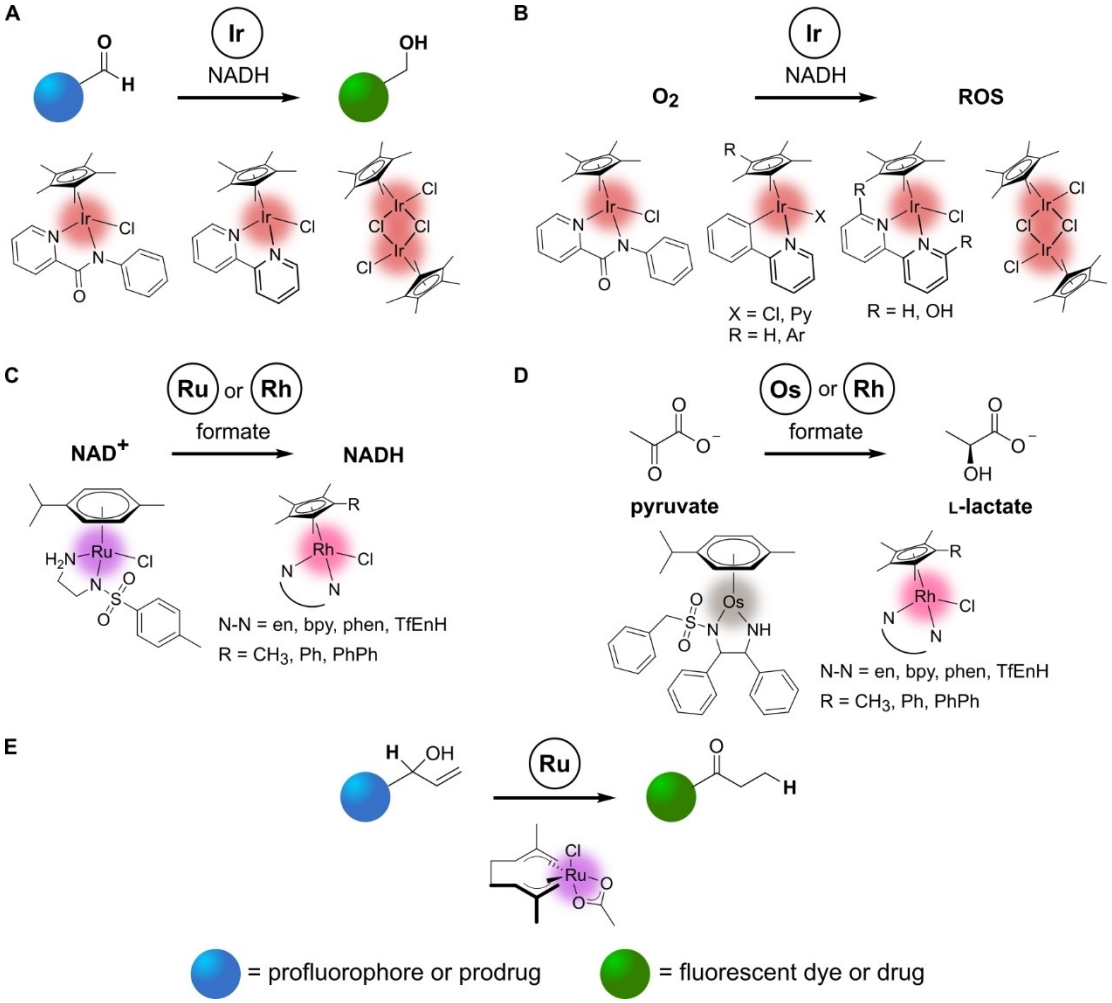

Figure 9. Overview of the transfer hydrogenation reactions carried out in cells. (a) Iridium catalysed hydride transfer reaction from NADH to aldehydes to give alcohols (Ref. [17]). (b) Iridium catalysed hydride transfer from NADH to oxygen to give ROS (Refs. [18–19]]). (c) Ruthenium and rhodium catalysed hydride transfer from formate to NAD^+ to give NADH (Ref. [22]). (d) Osmium and rhodium catalysed hydride transfer reaction from formate to pyruvate to give lactate (Refs. [23–24]). (e) Ruthenium catalysed intramolecular hydride transfer of allyl alcohols to give aldehydes (Ref. [26]).

then induce oxidative stress in the cell by producing peroxides and other ROS from O_2. Co-administering the iridium catalyst with the platinum complex appears to exhibit cytotoxicity even in platinum-resistant cancer cell lines.[19]

With ruthenium^{II} Noyori-type catalysts, formate has also been used as a hydride source to catalyse the reduction of NAD^+ to NADH (Figure 9d). Sadler et al. investigated a wide range of ruthenium complexes. The complexes were incubated in A2748 cells along with formate. The best complex, [(*p*-cym)Ru(TsEn)Cl], exhibited a decrease in cell survival from 69 % to just 1 %. This decrease in cell viability was due to the catalytic reduction of NAD^+, with the NAD^+/NADH ratio decreasing from 4.78 to 0.74, giving an apparent turnover frequency of $0.19 \pm 0.01\ h^{-1}$.[20]

Other metals are also able to catalyse the transfer hydrogenation reaction in living cells. Sadler et al. have demonstrated the use of rhodium and osmium complexes in vitro. Rh^{III} half-sandwich complexes (Figure 9c) were found to be active for the reduction of NAD^+ to NADH, and the reduction of pyruvate to lactate, using formate as the hydride source. The activity of the complexes towards altering the NAD^+/NADH ratio was investigated in A2780 cancer cells, with redox disruption in the cells leading to decreases in cell survival of up to 50 %.[21]

A chiral osmium (II) complex was found to successfully carry out the asymmetric reduction of pyruvate to lactate using formate as a hydride source in living cells (Figure 9c). The reduction was carried out in A2780 cancer cells; the significant decrease in cell proliferation of around 85 % was independent of the enantiomer of the complex used, although the enantioselectivity was maintained in vitro, and the activity of the catalyst was estimated to carry out around 13 TONs. The precise reason for the cell death is not clear, as up to 2 mM concentrations of either enantiomer of lactate are non-toxic, implying that the lactate production is unlikely to be the source of cell death, although perturbing local concentrations may still have an knock-on effect for other cell pathways. Furthermore the reactivity of the complex with other cellular components was unknown, meaning that other unsaturated endogenous substrates may be targeted as well.[22] In order to gain more insight into the system, the authors went on to investigate the intracellular stability of the complex. A brominated analogue of the complex was synthesised, which was shown to have the same reactivity and properties as the original complex. It was then possible to follow the brominated complex in cells using a combination of inductively coupled plasma mass spectrometry (ICP-MS) and nanoscale synchrotron X-ray fluorescence (XRF) mapping in order to gain insight into the cellular uptake and mechanism of the complex. From these analyses it was deduced that the catalyst is in fact degraded within cancer cells, by transport into acidic lysosomes followed by reaction with cellular thiols. They then determined that the ligand was detached from the osmium centre, and transported into the nucleus, without the osmium.[23]

Finally, a redox neutral intramolecular hydride transfer reaction has been explored *in vitro* using a Ru^{IV} complex (Figure 9e). A ruthenium bis-allyl complex has been used for the isomerisation of allyl alcohols to ketones. Analogous to the previous transfer hydrogenation reactions, a metal-hydride intermediate is required for intramolecular hydride transfer. This reaction displayed good reactivity in HeLa, A549, and Vero monkey kidney epithelial cells, as indicated by large increases in fluorescence intensity for the synthesis of a naphthalene-based dye. The reaction was even quantified by liquid chromatography mass spectrometry (LC-MS) analysis of methanolic extracts of the cells, revealing a calculated TON of 22.4 when 10 mol % of ruthenium complex was applied. This isomerisation reaction was then used to generate GSH-depleting compounds. A decrease in the intracellular glutathione concentration was observed after the ruthenium catalysed formation of *α,β*-unsaturated ketones, by exploiting their Michael type reactivity towards thiols. Using 50 mol % of catalyst in HeLa cells along with the bis-allyl substrate saw a 40 % decrease of glutathione levels.[24]

2.3. Bond Cleavage Reactions

2.3.1. Cleavage of terminal groups

Many of the early examples of transition metal catalysed reactions in living cells are deprotection reactions, whereby a small, terminal, protecting group is cleaved from the substrate. The desired property of the compound is then switched-on upon cleavage of the protecting group. Such reactions are useful for catalysis proof of concept, where deprotecting a profluorophore provides an easy method of monitoring the catalysis, by simply looking for an increase in fluorescence intensity. In addition, developing a range of deprotection reactions provides new possibilities for prodrug activation. While such reactions are dominated by ruthenium and palladium catalysts, examples with gold, platinum, and copper complexes are also known.

The [Cp*Ru(cod)Cl] complex has been used by several groups for *in vitro* allyloxycarbonyl (alloc) cleavage, whereby an allylcarbamate group is cleaved to produce either an amine or alcohol (Figure 10a), and was first used in cells by Meggers et al. to produce amines. Not only is the reaction tolerant to air and water, but it was found to require the presence of thiols in water. The catalyst was found to deprotect rhodamine 110 inside HeLa cells with 80 % yield, although 20 mol % of the complex was required, giving a modest TON of 4.[25] Building on this work, Mascareñas et al. used the same catalytic system for the deprotection of DNA-binding agents in CEF chicken embryo fibroblast cells and Vero cells. The DNA-binders displayed protection-dependent spectroscopic properties, providing a handle to determine successful catalysis. Low amounts of fluorescence corresponding to the protected binders was observed, while high levels of fluorescence was observed following incubation with the catalyst, indicating that catalysis had taken place, although quantification of the product was not provided.[26] The catalyst has also been deployed for controlled localised profluorophore activation, as well as localised prodrug activation. Rotello et al. deposited the

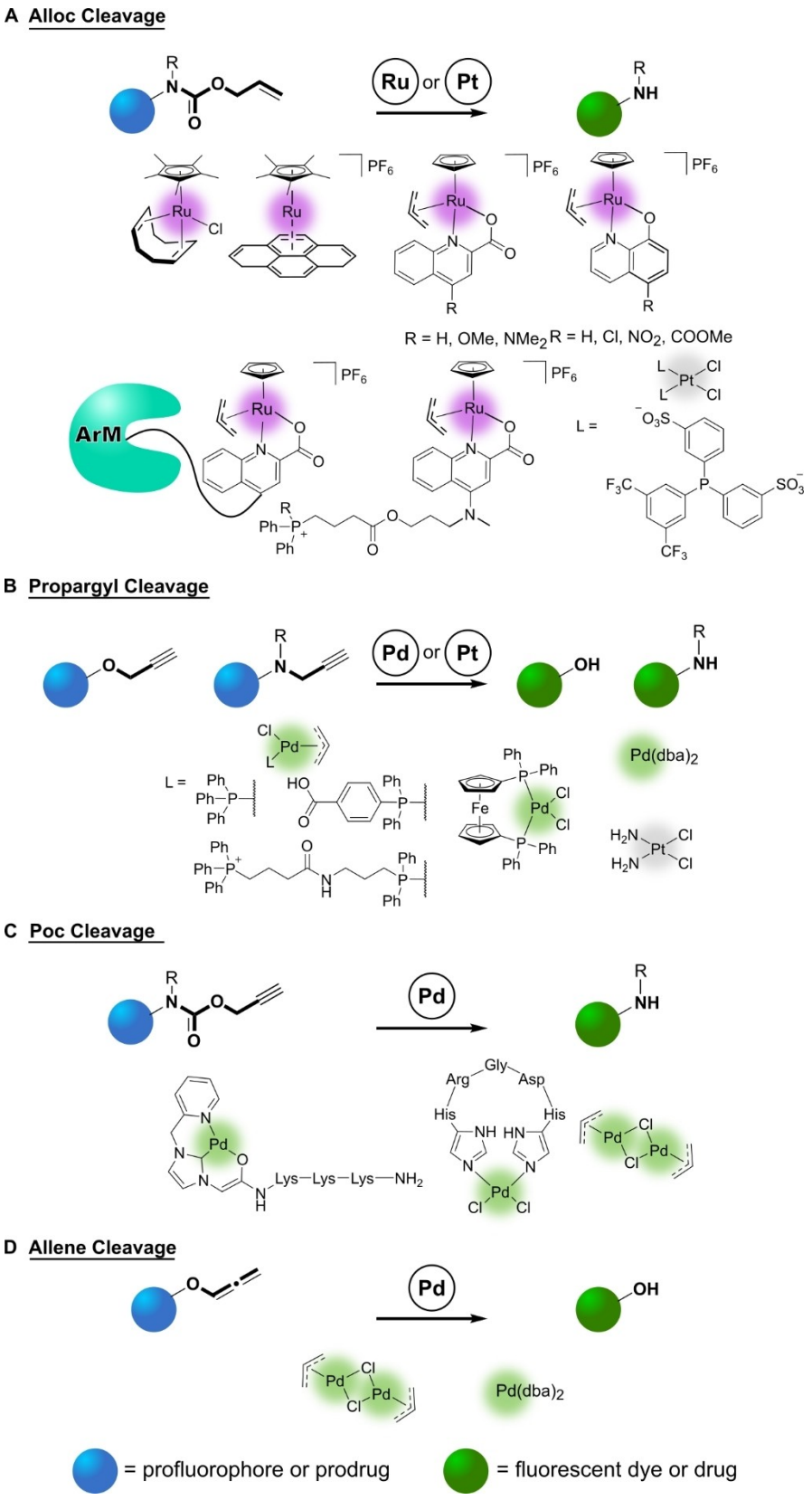

Figure 10. Overview of catalytic cleavage of terminal groups carried out in cells. (a) Ruthenium, and platinum catalysed alloc cleavage (Refs. [25–31,34]). (b) Palladium and platinum catalysed propargyl cleavage (Refs. [36–40]). (c) Palladium catalysed poc cleavage (Refs. [41–42]). (d) Palladium catalysed allene cleavage (Ref. [43]).

complex in between decorative monolayers on a gold nanoparticle to create a nanozyme (Figure 11). Nanoparticles decorated with cationic ammonium groups were able to penetrate the cell membrane, while zwitterionic nanoparticles remained extracellular, resulting in the concurrent, spatially controlled alloc deprotection of an anticancer prodrug, alloc-doxorubicin, in and outside HeLa cells. Successful deprotection was indicated by a decrease in cell viability, although the observed cell viability was not as low as for doxorubicin alone, indicating that full deprotection was not obtained.[27]

Also with a goal towards spatial control, Meggers et al. investigated a photoactivated version of the catalyst, [Cp*Ru(η^6-pyrene)](PF_6). Following irradiation with UV light, the pyrene moiety dissociates from the ruthenium, and the resultant complex can catalyse the deprotection of rhodamine 110. The reaction was carried out in HeLa cells, and resulted in a 70-fold increase in fluorescence intensity, indicating that catalysis was successful.[28]

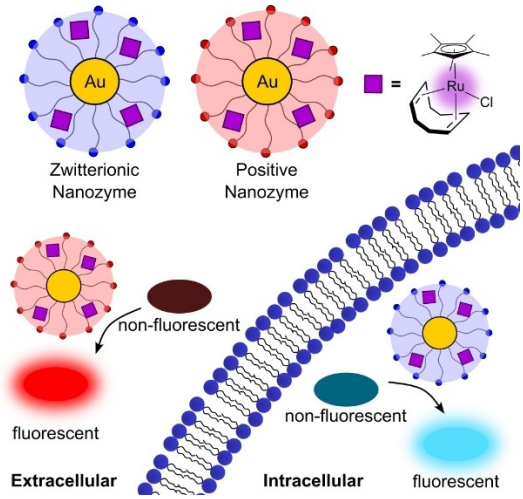

Figure 11. Schematic representation of the gold nanozyme containing the ruthenium catalyst. The zwitterionic nanozymes are cell impermeable and undergo catalysis in the extracellular space, while the positive nanozymes are cell permeable and are able to carry out catalysis inside the cell.

Several derivatives of this complex have been shown to successfully cleave alloc groups. Meggers et al. used ester and amine derivatives of the complex in order to be able to use the catalyst intracellularly in HeLa cells. When 20 mol % of the amine derivative was used in cells, catalytic deprotection of the anticancer drug doxorubicin was observed, as seen by a decrease in cell viability, although only around 10 % of the prodrug was activated.[29] In contrast, the activity of the ester derivative towards doxorubicin activation in HeLa cells was increased 10-fold.[30] The catalyst scaffold was further functionalised with a mitochondria-targeting moiety by Mascareñas et al. The presence of a cationic phosphonium group is required for accumulation within the mitochondria; however, this appears to make it a less active catalyst, as rhodamine 110 deprotection in water had a yield of only 14.2 %. In the presence of lysates it was barely active, with just 0.2 % yield. Even so, the complex was used for the activation of 2,4-dinitrophenol (DNP), a compound known to decrease the mitochondrial membrane potential and switch off ATP production, in HeLa and Vero cells. Indeed activation of the compound appeared to take place, by an observed decrease in the mitochondrial membrane potential.[31]

Biotinylated derivatives of this catalyst have also been used by Ward et al.. They generated a cell-penetrating artificial metalloenzyme by docking the catalyst inside streptavidin alongside a fluorescent cell-penetrating polymer. Streptavidin is a protein that has an astonishingly high affinity for biotin, a small vitamin.[32] Streptavidin has four binding sites that bind biotin with hydrogen bonding and van der Waals interactions. This binding is one of the strongest non-covalent interactions found in nature, and is much stronger than typical protein-ligand interactions.[33] This therefore makes streptavidin highly useful as a host for the generation of artificial metalloenzymes, as biotinylated metal complexes are able to be docked within the protein with great ease. The artificial metalloenzyme was used to regulate a gene switch in HEK-293T cells: ruthenium mediated alloc cleavage generated the thyroid hormone T_3, which upregulates a gene circuit that leads to the production of a bioluminescent reporter (Figure 12), providing a way by which the catalysis can be monitored; indeed, increased luminescence intensities were observed in the presence of

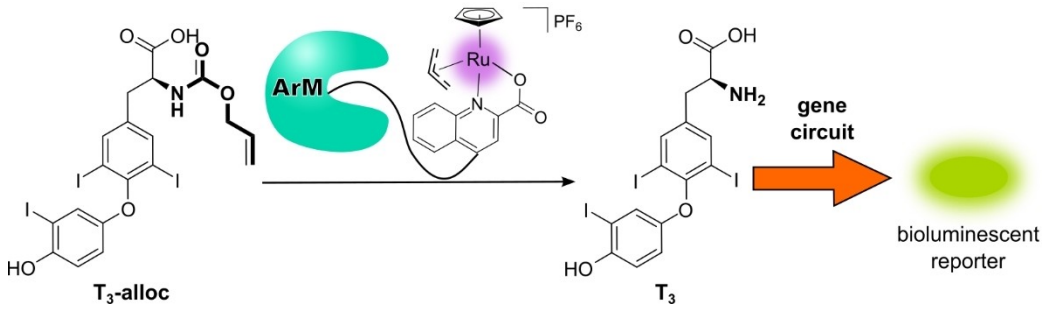

Figure 12. The artificial metalloenzyme containing a Tsuji–Trost ruthenium catalyst catalyses the alloc deprotection of thyroid hormone T_3, which upregulates a gene circuit that produces a bioluminescent reporter. The luminescence intensity of this reporter can be used to monitor the catalysis.

the ruthenium complex, with better activity seen for the artificial metalloenzyme than for the free catalyst alone.[34]

Palladium complexes are well suited for the deprotection of propargyl groups, to form amines and alcohols. With the intention of developing a palladium-sensing system that could be applied in living systems, a propargyl-protected fluorescein was synthesised that could be used as a switch-on fluorescence system to detect the presence of palladium. 5 day old zebrafish were incubated with 20 μM of the probe, and as little as 5 μM of $PdCl_2$ resulted in fluorescence, indicating that the cleavage was successful.[35] A series of Pd^0 and Pd^{II} allyl complexes have also been used for the deprotection of a propargyl-protected profluorophore, in Vero cells. The Pd^0 complexes were inactive for the deprotection of the propargyl group in the presence of cell lysates; however, the Pd^{II} complexes were able to generate the deprotected product in up to 10% yield. When the reaction was then applied in the Vero cells, estimated average TONs of 5–10 were observed.[36]

Prodrugs can also be protected with this propargyl group. A discrete palladium complex deposited in between monolayers on a gold nanoparticle also catalyses the deprotection reaction (Figure 13). Here, catalysis is controlled by supramolecular strategies. Cucurbit[7]uril (CB[7]) binds to the terminal monolayers, and the steric hindrance inhibits catalysis. However, after addition of 1-adamantylamine (ADA) as a competitive guest, the CB[7] dissociates from the nanoparticle to bind the adamantylamine, and frees up space for the catalysis to take place. This Pd-NP system exhibited this gated catalytic behaviour in HeLa cells with prodrug activation. After 48 h, most of the anticancer compound 5-fluorouracil (5FU) was activated.[37]

Alternatively, a simple $Pd(dba)_2$ complex applied in stoichiometric amounts was shown to activate NO-releasing prodrugs. Upon cleavage of the propargyl group, the free diazeniumdiolates spontaneously release NO, which is known to induce cell death. The antiproliferative activity of 1 μM of prodrug was analysed with and without the palladium complex in a variety of cell lines. A significant enhancement in antiproliferative activity was observed in the presence of 1 μM of palladium. The authors also observed a small improvement in the presence of only 0.25 μM, indicating that the reaction can be catalytic in metal complex. Control reactions with an NO-sensitive fluorophore showed that NO was produced in the presence of palladium, indicating that the mechanism of antiproliferation indeed occurred through deprotection of the propargyl group and subsequent liberation of NO.[38]

Platinum complexes have also been utilised as a deprotecting agent in cancer cells, with dual-action toxicity from both the released prodrug and from the active platinum complex itself (Figure 14). In this novel deprotection strategy, a propargyl-caged NO releasing prodrug is covalently linked to a "masked" Pt^{IV} complex. This compound is stable and non-toxic in healthy cells; however, cancer cells reduce the Pt^{IV} complex to Pt^{II}, resulting in the release cisplatin. The free cisplatin then induces cancer cell death through two mechanisms: 1) it can enter the nucleus and form a platinum-DNA adduct, and 2) it can catalyse the propargyl deprotection of the prodrug. This deprotection results in the release of two molecules of toxic NO. Since one molecule of cisplatin is released from every prodrug molecule, the platinum complex is present in stoichiometric amounts with respect to the prodrug. Although not catalytic, the platinum complex was successfully able to mediate prodrug activation in cancer A549 cells. Interestingly, the antiproliferative activity of the Pt-prodrug compound was much greater in cancer cells compared to human normal ovarian epithelial IOSE80 cells, with a selectivity factor of 518. This was attributed to the fact that cancer cells have a sufficiently reductive environment to reduce the Pt^{IV} complex to cisplatin, whereas healthy cells are unable to reduce the Pt^{IV}

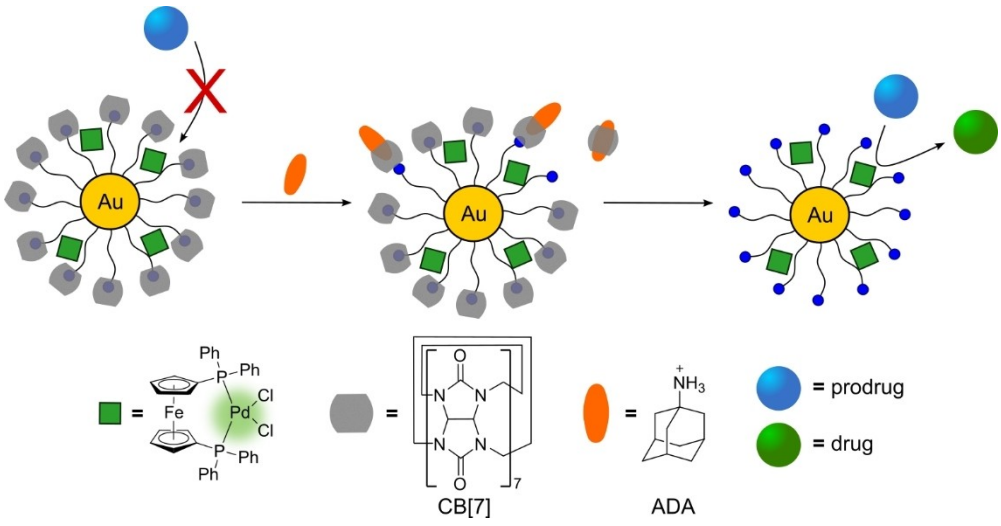

Figure 13. Schematic representation of the gold nanoparticle with the ruthenium catalyst deposited in between the monolayers, and the monolayers capped with CB[7]. Pd-NP is able to catalyse the activation of a prodrug in cells. When CB[7] is bound to Pd-NP it is unable to catalyse the transformation as steric hindrance prevents the substrate from reaching the catalyst. However, when ADA is added the CB[7] leaves the nanoparticle and instead binds the ADA, providing space for the catalysis to take place again.

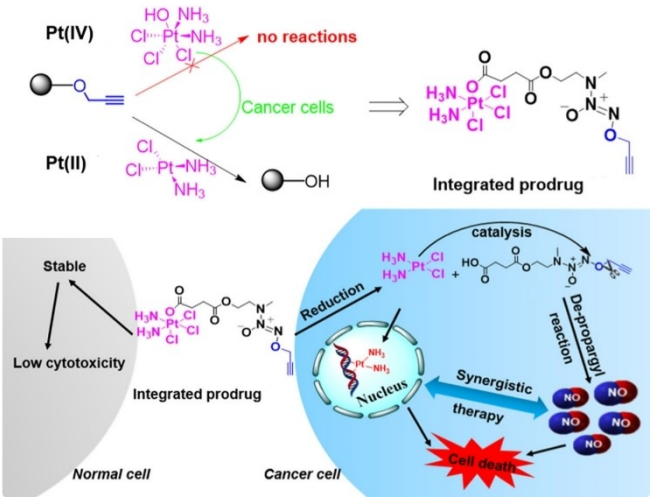

Figure 14. Dual-action toxicity of an NO-releasing prodrug bound to a platinum complex. In normal cells, the Pt^{IV}-prodrug complex is stable and induces low levels of cytotoxicity. However, the reductive environment of cancer cells is sufficient to reduce the Pt^{IV} to Pt^{II}. This results in the release of cisplatin from the prodrug, which is then able to cleave the propargyl group. The activated drug then releases NO that induces cell death; in parallel, the cisplatin enters the nucleus and forms a platinum-DNA adduct, which also induces cell death. Reproduced with permission.[39] 2020, ACS Publications.

complex and it remains in its inactive form. This cell selectivity was also observed in a xenograft zebrafish model, where the Pt-prodrug compound was shown to be stable in vivo, and only activated in the cancer cells.[39]

Another commonly used alkyne-containing terminal protecting group is the propargyloxycarbonyl (poc) group. Similar to the alloc protecting group, cleavage of the poc group generates an amine (Figure 10c). Pd^{II} metallopeptides are known to catalyse the cleavage. A carbene-based catalyst was connected to a cell-penetrating peptide, to make the complex able to enter PC-3 human prostate cancer cells. Once inside the cells the complex mediated the deprotection of rhodamine 110, with flow cytometry analysis showing an increase in fluorescence intensity, indicating the formation of the fluorophore.[40] A bis(histidine) complex made use of arginines to aid cell internalisation. Here, the palladium forms a bridge to join together two histidine residues on a small protein, inducing conformational strain on the peptide chain. The peptide complex catalyses the deprotection, while the free palladium source does not. The reaction is helped by the strained metal bridge, and the protein scaffold provides some protection against metal deactivation. The complex was able to mediate the deprotection of fluorescent probes in a variety of cancer cells.[41] Palladium complexes have also been shown to catalyse one other type of deprotection reaction, namely cleavage of an allenyl group from protected amino acids (Figure 10d). Pd^{II} complexes were investigated for their deprotection activity towards allenyl-protected tyrosine residues on green fluorescent protein in HEK293T cells. The complexes were able to successfully deprotect the tyrosine residues, and were found to mediate the reaction with yields of up to 51 %. The catalysts were then further applied to gain-of-function of an enzyme within cells. When tyrosine residues in the active site of the anthrax lethal factor, the key toxin effector from *B. anthracis*, are protected with allenyl groups, the enzyme is inactive. However, after incubation with the palladium complexes, the activity of the enzyme was restored.[42]

2.3.2. Cleavage of internal groups

Although the most common example of metal-mediated bond cleavage reactions in cells is the deprotection of a small terminal groups, there are also a growing number of examples where internal linker groups are cleaved. These linkers find themselves joining together a drug or prodrug with a second targeting group. One application of bifunctional linkers is to attain spatial control over prodrug activation. Drugs can be linked to an antibody, to form a large structure known as an antibody drug conjugate (ADC). The antibody behaves as a targeting group, as the selected antibody will dock into the desired complementary antigen and bring the drug to the desired location. However, if instead an inactive prodrug is used, cleavage of the linker group then liberates the activated drug, resulting in selected activation of the prodrug only at the desired location.

The versatility of this ADC system was demonstrated by Chen et al. using a Cu^{I} complex. Following a very large screening, the authors identified the complex Cu-BTTAA as being the most active towards propargyl cleavage from protected amines and phenols (Figure 15). The Z_{HER2} affibody (a small peptide that targets the HER2 receptor) was selected as the bioconjugation partner. Drugs containing an amine (doxorubicin) and a phenol (Etoposide) were linked to this affibody through the propargyl linker. For both drugs, after incubation in SKBR-3 cells the addition of a stoichiometric amount of copper complex (20 eq. and 1 eq. respectively) resulted in toxicity levels comparable to the free drugs, indicating the successful cleavage of the linker. This linker cleavage was then further used for reversible cell surface modifications. The propargyl linker was used to bind biotin to the surface of A549 cells. Incubation of the cells with fluorescently-labelled streptavidin resulted in strong fluorescence at the cells surface, due to the strong biotin-streptavidin binding. However, incubation with 20 eq. of copper complex resulted in the almost complete disappearance of fluorescence at the cell surface after only 1 h, which again indicates successful cleavage of the linker from the cell surface. Finally, the linker was also used for reversible protein mutagenesis, in order to provide a handle for modulating protein interactions. Site-selective protein modifications were achieved by incorporation of propargyl-caged lysine and tyrosine into a fluorescently-labelled Z_{HER2} affibody. While the native affibody binds to the HER2 receptors, resulting in strong fluorescence at the surface of SKBR-3 cells, when the modified Z_{HER2} containing the protected amino acid residues was used no fluorescence was observed, indicating a lack of binding. However, treatment with 10 μM of copper complex restored the fluorescence, showing that Z_{HER2}-HER2 binding can be controlled by the

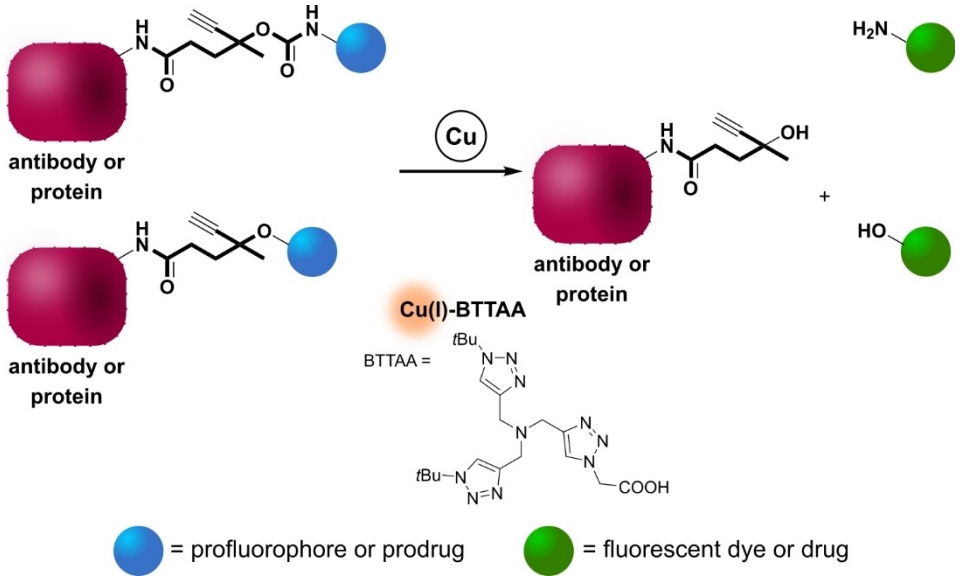

Figure 15. Copper catalysed cleavage of internal linkers. Cleavage of an ADC generates amine-containing and hydroxyl-containing drugs.

cleavage of propargyl protecting groups from protein residues.[43]

2.4. Cyclisation Reactions

2.4.1. Intramolecular hydroarylations and hydroalkylations

Au^{I} complexes are well known for their reactivity towards cyclisation reactions. Mascareñas et al. used a Au^{I} 1,3,5-triaza-7-phosphaadamantane (PTA) complex, [AuCl(PTA)], to carry out a hydroarylation cyclisation catalytically in cells (Figure 16a). The hydroarylation of procoumarin was investigated, in order to monitor catalysis by fluorescence. As gold is known to form strong bonds with thiols, the bioorthogonality of the reaction was first investigated in the lab. Although with 10 mol % of gold complex in the presence of 1 eq. of some intracellular thiols (methionine, cytosine, histidine) high yields of 71–94 % were still obtained, in the presence of other intracellular thiols (glutathione, cysteine or adenine) no yield was observed. Nevertheless, the gold complex was still able to generate an aminocoumarin derivative in the presence of cell lysates and bacteria, with yields of 27 % and 12 % respectively. The reaction was further applied to HeLa cells, where a large increase in fluorescence intensity was seen after incubation of the profluorophore with the gold complex. Although the reaction was clearly able to take place inside cells, the reaction appears to be sub-stoichiometric, with a reported estimated TON of 1.12. Interestingly, it was also shown that this hydroarylation reaction could also occur concurrently in HeLa cells alongside a ruthenium catalysed deallylation reaction.[44]

Conversely, Zou et al. used this strong thiol-gold interaction to their advantage by showing targeted anti-cancer activity of organogold(I) complexes in cancer cells and zebrafish. In order to achieve controlled activation of the catalyst, the authors designed a system in which an inactive gold complex undergoes a transmetallation reaction with palladium in order to generate a gold-chloride species (displayed in Figure 16a) that is both catalytically active towards intramolecular alkyne hydroarylation, and cytotoxic towards cancer cells. A stable, non-toxic gold pre-catalyst is activated upon transfer of a phenylacetylene ligand to a Pd^{II} complex, which then undergoes reductive elimination to produce 1,4-diphenylbuta-1,3-diyne and a Pd^{0} species. The resultant gold species was then able to catalyse the cyclisation of a procoumarin derivative to generate the fluorescent product. Although this process occurred very efficiently in organic solvent with up to 96 % yield, a large decrease in yield was observed when the reaction was moved to PB or PBS. Nevertheless, the authors demonstrated that their palladium-activated system showed much greater reactivity in the presence of 1 eq. of glutathione compared to the reaction with the analogous "pre-activated" complex. In addition, when the substrate, gold complex, and palladium complex were incubated in A549 cells notable fluorescence was observed in the cytoplasm, which was not seen for any of the components alone. The reaction was then further successfully applied inside zebrafish with similar results, although in neither case was the fluorescence quantified. As well as being catalytically active, the resultant gold complex was also shown to induce cytotoxicity in a range of cancer cells, by binding to thiol-containing enzymes, thioredoxin reductases, and inhibiting their function. This cytotoxicity was targeted towards cancer cells over healthy cells, by using a palladium source that was bound to a small stapled peptide, which targets integrin-overexpressing cancer cells. When the gold-palladium system was applied to HeLa cells considerable cell death was observed, while healthy cells with low integrin-expression remained viable. Zebrafish have been shown to be a good model to

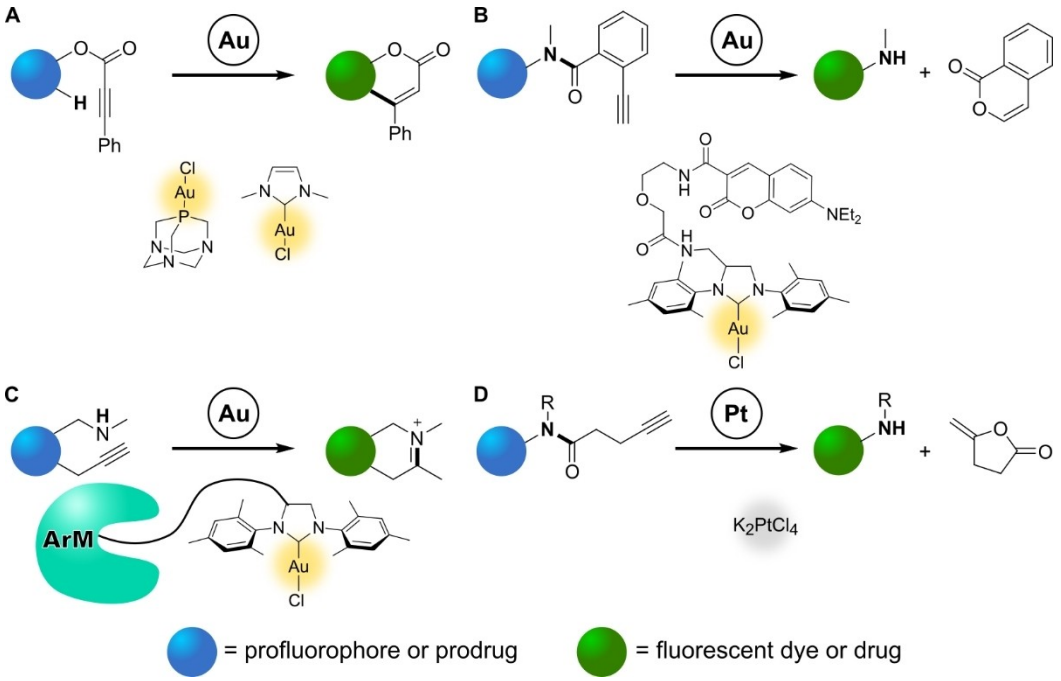

Figure 16. Overview of catalytic cyclisation reactions carried out in cells. (a) Gold catalysed intramolecular hydroarylation (Refs. [44–45]). (b) Gold catalysed intramolecular hydroarylation to induce cleavage of a protecting group (Ref. [46]). (c) Gold catalysed intramolecular hydroamination (Ref. [47]). (d) Platinum catalysed intramolecular carbocyclisation to induce cleavage of a protecting group (Ref. [48]).

study tumour angiogenesis, so therefore the gold-palladium system was again applied in zebrafish. It was observed that blood vessel formation was impaired by the activated gold complex while the gold complex or palladium complex alone did not, demonstrating that this form of gold activation may be useful for improving spatiotemporal specificity of catalysis in cells.[45]

Instead of directly using this type of cyclisation reaction as a tool for the synthesis of fluorophores or prodrugs, intramolecular hydroarylations have also been used as a method of bond cleavage for application in deprotection reactions (Figure 16b). To this end, a Au^I complex has been used to deprotect prodrugs through the cyclisation of a 2-alkynylbenzamide (ayba) protecting group. Following the cyclisation, a drug is released via the formation of a secondary amide, as well as the ring closed by-product. Control reactions in the lab demonstrated that a gold-NHC complex was most active for this reaction, as 1 eq. IPrAuCl successfully mediated the activation of ayba-protected endoxifen. Interestingly, this deprotection was also able to take place in parallel to the deprotection of alloc-protected and propargyl-protected doxorubicin by ruthenium and palladium complexes respectively, showing that this gold-mediated deprotection has the potential to be used orthogonally to other deprotection reactions. Due to solubility reasons, a coumarin-modified analogue of the catalyst was used for reactions *in vitro*, which was used for the deprotection of ayba-protected doxorubicin. In multiple cancer cell lines (HeLa, A549, and PC3) a significant decrease in EC_{50} values was observed when the prodrug was incubated in the presence of stoichiometric quantities of the gold complex.[46]

In order to protect a gold catalyst from thiol poisoning, an artificial metalloenzyme containing a gold complex was developed, whereby a coumarin-modified NHC-Au^I complex was docked inside an albumin scaffold in order to catalyse hydroamination reactions of 5-methyl phenanthridinium derivatives (Figure 16c). A bioorthogonality screening revealed the protective role of the protein scaffold: while the free complex exhibited almost no activity in the presence of glutathione or cell lysates, only a slight decrease in activity for the artificial metalloenzyme was observed, with high TON still obtained. The artificial metalloezyme was then shown to be active in the cyclisation of a prodrug, in order to synthesise a cytotoxic anticancer compound. While low catalyst loadings gave moderate yields, at 20 mol % of artificial metalloenzyme full conversion could be achieved. When the reaction was then applied inside A549 cancer cells, the protective nature of the protein host was further demonstrated. The metalloenzyme was more efficient at prodrug activation than the free gold complex, as it was observed that only 0.63 μM of metalloenzyme was required to achieve a decrease in cell growth by 50 %, whereas 2.5 μM of free complex was needed to reach the same level. Interestingly, it was also observed that docking of the gold complex inside the protein scaffold reduced its cytotoxicity compared to the free complex.[47]

Gold complexes are not the only players in mediating cyclisations in cells. Platinum complexes have also been shown to be active for intramolecular carbocyclisations (Figure 16d). Simple platinum salts have been used in cells

to combine a carbocyclisation with the release of a secondary amine-containing drug. Following a carbocylisation of an alkyne-amide or alkyne-carbamate, a lactone is released, while simultaneously generating a free amine. Although control reactions showed that cisplatin and K_2PtCl_4 could successfully deprotect alkyne amides or carbamates from secondary amines at catalytic quantities in water, a large stoichiometric excess of platinum complex was required for reactions in cells. The deprotection of an antineoplastic drug, MMAE, and anticancer drug, 5FU, was shown to proceed in HeLa cells. After incubation with the non-toxic prodrugs of MMAE (1 nM) and 5FU (100 μM), a 2-fold increase in toxicity was observed following the application of 20 μM of K_2PtCl_4 twice a day for three days. Despite this large amount of platinum added to the cells, the authors noted that in both cases the toxicity of the unmodified drugs was not reached, which indicates that even after 3 days full conversion to the deprotected drugs was not obtained. It is likely that glutathione was the root of this poor activity, as control reactions in the lab with 50 eq. of platinum complex in the presence of 1.5 mM glutathione resulted in reduced conversions, although the reaction rates were still good. Nevertheless, MMAE was also shown to be successfully deprotected from an ADC, whereby an alkyne amide linker was used to conjugate the MMAE to the F16 antibody, which is known to specifically bind to the tenascin-C receptor, and which is overexpressed in cancer cells. Again, large excesses of K_2PtCl_4 resulted in the liberation of MMAE from the ACD in HeLa cells. Finally, cisplatin was successfully applied in the formation of 5FU in zebrafish. Colorectal cancer (CRC) HCT116 zebrafish xenografts were generated for incubation with protected 5FU (1.65 mM) and cisplatin (34 μM). After 6 days, a significant decrease in tumour size was observed.[48]

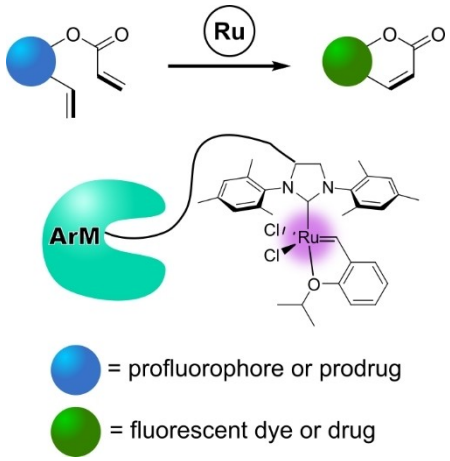

Figure 17. Ruthenium catalysed ring closing olefin metathesis (Ref. [51]).

2.4.2. Ring closing metathesis

Olefin metathesis is an extremely versatile reaction, with ring-closing metathesis, cross-metathesis and ring-opening polymerisation catalysis providing a means to access a wide range of useful products, notably for pharmaceutical production.[49] Therefore it is not surprising that the pursuit of applying this reaction in living cells is of great interest. Indeed metathesis has been effectively used for protein modification.[50] However, to date there have only been a handful of examples of the reaction being applied in living cells, and they have all made use of the ArM strategy (Figure 17).

An artificial metalloenzyme developed for metathesis reactions used a coumarin-modified Hoveyda-Grubbs second generation catalyst docked inside of albumin. The length of the linker between the coumarin and the NHC ligand was optimised such that the complex resided within the hydrophobic pocket of the protein, and was therefore protected from thiol poisoning, as the hydrophilic intracellular thiols would be repulsed by the apolar nature of the cavity. Having optimised the structure of the ligand, it was shown that the complex could undergo ring closing metathesis with no reduction in activity in the presence of up to 20 mM glutathione. After decorating the exterior of the albumin with α(2,3)-linked sialic acid targeting groups, the artificial metalloenzyme was shown to accumulate in SW620 colon adenocarcinoma cells, by binding to overexpressed galectin-8 receptors. In the presence of these cells, the cyclisation of a prodrug to generate a cytotoxic compound was carried out, whereby cell growth could be decreased to $<5\,\%$, while the artificial metalloenzyme without the targeting groups was much less active at inducing cytotoxic effects. While this observation made it clear that the targeting is important for the prodrug activation, it was not clear if this activation was taking place on the cell surface, or intracellularly.[51]

2.5. Cyclo-addition Reactions

Alkyne-azide cycloadditions have long been known for their excellent bioorthogonality, as neither alkynes nor azides are endogenous to living systems, and typically both substrates, as well as the stable triazole product, exhibit low levels of cytotoxicity. In addition, fast reaction kinetics and high yields make such reactions very applicable to cellular conditions. The copper catalysed variant of this cycloaddition (CuAAC) provides a means to access an extraordinarily broad substrate scope. The reaction requires a Cu^{I} catalyst, which is usually generated in situ from a Cu^{II} source and reductant, most commonly $CuSO_4$ and sodium ascorbate, with a wide variety of ligands that have been used (Figure 18).

Cai et al. showed protein labelling using the CuAAC reaction with a coumarin dye, both on the cell surface and intracellularly, with a cell-penetrating peptide attached to the tridentate triazole ligand to ensure entrance of the complex into the cell. While the surface labelling took place with a very modest yield of 18 %, inside the cell a yield of only 0.8 % was achieved. This low yield was attributed to the presence of catalyst-poisoning thiols.[52]

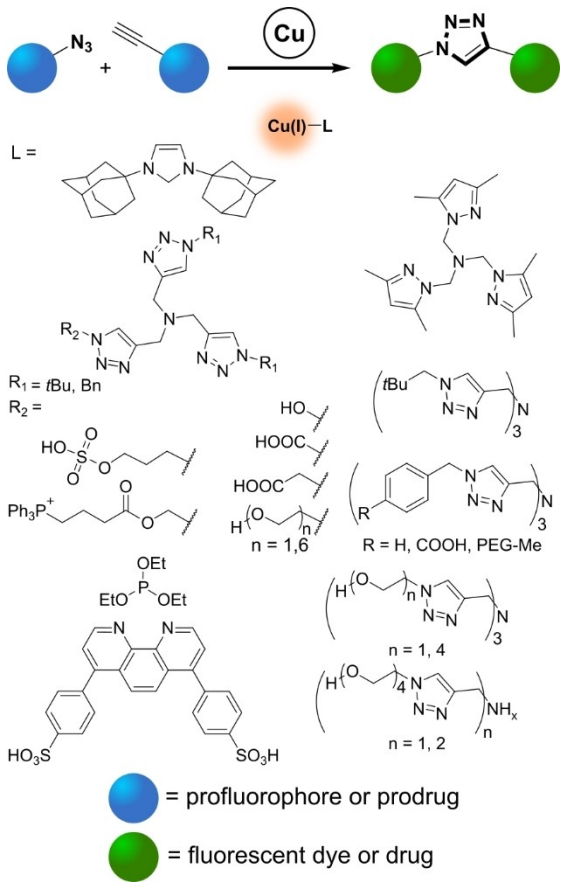

Figure 18. Overview of copper catalysed alkyne-azide cycloadditions carried out in cells (Refs. [52–54]).

CuAAC chemistry has also been used for small molecule synthesis in vitro. Mascareñas et al. achieved the synthesis of a fluorescent anthracene derivative inside of mammalian cells. Although the obtained yields were not high, with a maximum yield of 18 %, the reaction was able to proceed without the addition of any external reducing agent.[53]

Interestingly, Mascareñas et al. also showed that ruthenium complexes can be used for the azide-thioalkyne cycloaddition reaction under biorelevant conditions.[54] They also reported analogues of the complex that are active after photoactivation, providing opportunities for optobiology.[55] In addition, also the (2+2+2) cycloaddition of alkynes has been reported in live mammalian cells using ruthenium complexes.[56] Finally, iridium complexes may also be a viable candidate for cycloadditions in cells in the future, as an iridium^{II} complex has also been used under biologically relevant conditions for an ynamide-azide cycloaddition,[57] hydroxylalkyne-azide cycloaddition,[58] and disulfide-azide cycloddition.[59]

2.6. Cross-Coupling Reactions

Palladium catalysed cross-coupling reactions are extremely useful tools for achieving carbon-carbon bond formations in organic synthesis. Therefore, it is no surprise that achieving this reactivity inside living cells is of great interest, as it would provide access to the in situ synthesis of a wide range of drugs. The Sonogashira cross-coupling reaction couples together terminal alkynes with aryl halides to generate acetylene derivatives (Figure 19a). The palladium catalysed reaction typically uses a Cu^{I} co-catalyst and the presence of amines, although there are many examples of copper-free reactions.[60] All examples of the Sonogashira reaction applied in the presence of cells have used a copper-free system, although the reaction is yet to be carried out catalytically, as these first examples of the transformation *in vitro* required not just stoichiometric amounts of palladium

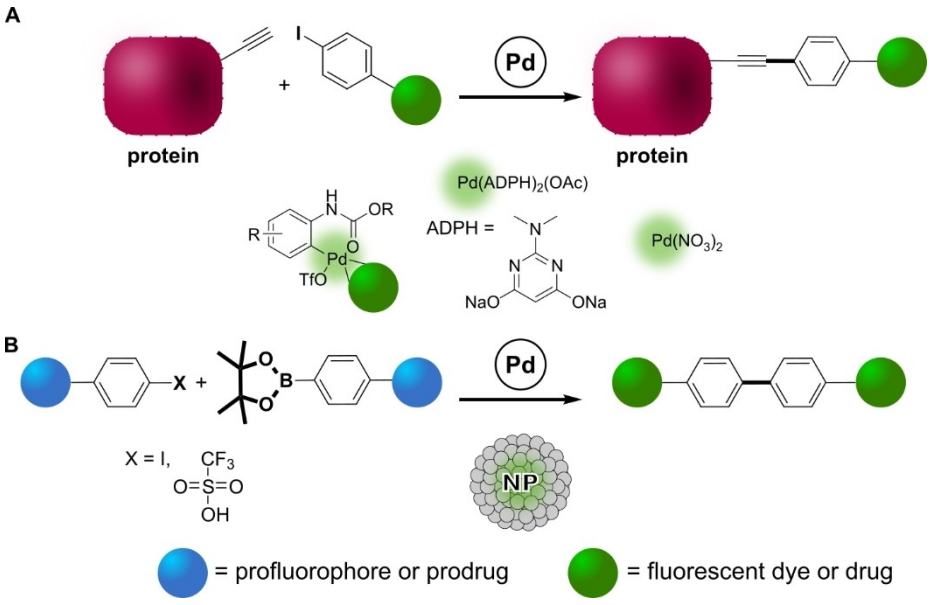

Figure 19. (a) Palladium catalysed Sonogashira couplings (Ref. [61]). (b) Palladium catalysed Suzuki–Miyaura couplings (Ref. [62]).

complexes, but even large excesses with respect to the alkyne.[61]

The Suzuki–Miyaura reaction is a different kind of palladium catalysed cross-coupling reaction, which typically couples aryl halides to aryl boronic acids or esters (Figure 19b). Palladium nanoparticle-containing microspheres have been shown to catalyse Suzuki–Miyaura reactions in mammalian cells. This is the first example of a non-enzymatic aryl-aryl bond formation to have taken place inside a living cell.[62] Other palladium nanoparticles are also active for fluorophore and drug syntheses.[63]

2.7. Other Reactions

In the only example of a gold mediated reaction that does not involve a cyclisation, Tanaka et al. made use of an artificial metalloenzyme containing a gold complex to conduct propargyl ester amidation in live mice. The artificial metalloenzyme was comprised of a coumarin-modified cyclometallated Au^{III} complex that was docked inside of glycoalbumin (Glyco). Depending on the specific N-glycan structure used, the Glyco-Au adduct is able to target specific organs, specifically α(2–6)-disialoglycoalbumin (Sia) for targeting the liver, and galactosylglycoalbumin (Gal) for the intestine. After injection of the Glyco-Au complex into the mice, it selectively accumulates in an organ. Subsequent injection of a fluorescent propargyl ester results in gold-catalysed organ labelling, by forming amide bonds with surface amino groups on the tissue (Figure 20). Control reactions in the lab with 10 mol% of Glyco-Au complex with a lysine residue on the albumin in a H_2O/DMSO mixture resulted in the conjugation of about six fluorescent molecules to the protein after 20 h; oddly enough, no further control reactions are given, neither in biological media, nor in cells. Despite this, an increase in fluorescence intensity is observed in the mice, which is localised around the target organs, and which indicates that the reaction took place.[64]

3. Compatibility Challenges and Potential Future Strategies

The reactions that have been carried out in living cells range from simple redox transformations, to intramolecular bond breaking and bond making reactions, and to challenging intermolecular coupling reactions. In general, the main problems observed for almost all these reactions include: 1) inhibition of the metal complex, resulting in stoichiometric rather than catalytic transformations; 2) a lack of selectivity, where the metal complex can react with non-desired substrates or activate prodrugs at a non-desired location; and 3) a lack of predictability of how the metal complex will behave in cells. In addition, it is hard to quantify the amount of catalyst in the cell and its location within the cell, and also the lifetime of its presence, as it could be excreted by, for example, endosomal excretion. Also the translation of the results of control reactions in the lab (in aqueous buffers or in the presence of biomolecules) to the application in cells is complicated. In some examples the control reactions indicate that the catalyst is completely inhibited by biomolecules; however, when the same system is then applied in living cells, there is clear evidence that the reaction does take place. Therefore, the development of reliable screening protocols in the lab that better replicate the environment of the cell are necessary to understand the problems faced in cells.

A diverse range of transition metal catalysts and reactions have been shown to exhibit some degree of compatibility with living cells. While precise control over the reactivity of small metal complexes as catalysts is possible, for example by simple modifications to the ligand structure, the metal centre is often highly exposed to the cell environment and can be readily deactivated. Harder first row transition metal complexes may be less susceptible to deactivation by soft thiol-containing biomolecules than softer second and third row metal complexes, but many of these first row metals are native to cells inside endogenous metalloenzymes.[65] This means that the desired reaction may be catalysed by endogenous metals as well as (or

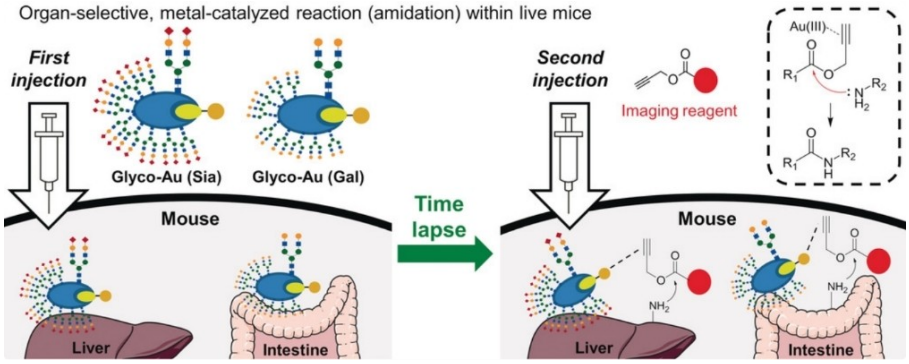

Figure 20. A gold catalyst docked inside glycoalbumin (Glyco-Au) is able to target either the liver or the intestines in mice depending on the nature of N-glycan structure used. The Glyco-Au adduct was first injected in live mice. A fluorescent propargyl ester is then also injected into the mice, and amino acid residues on the surface of the organs are labelled by the Glyco-Au adduct. Reproduced with permission.[64] 2017, Wiley Publishing.

instead of) the intended artificial metal complex, resulting in non-specific reactivity, as well as complicating analysis of the reaction. Although the use of second and third row transition metal catalysts comes hand in hand with biomolecule poisoning, their catalytic reactivity is superior for their application in cells, and searching for new strategies to prevent this poisoning is definitely worthwhile. While the reactivity of transition metal catalysts that has been achieved up until now is impressive, significant improvements on the biocompatibility of the metals with the cell environment need to be achieved in order to make future progress in the field of transition metal catalysis in living cells. Artificial metalloenzymes can provide protection from biomolecule inhibition, and provide a route to targeted catalysis, for example by overexpressing the protein host in a particular location of the cell, such as the periplasm. This may, however, involve large amounts of screening and protein evolution experiments to find the optimum artificial metalloenzymes. Although artificial metalloenzymes are in principle a viable strategy to overcome some of the problems faced in cells, the number of artificial metalloenzymes applied in living cells is still very low compared to that of discrete molecular catalysts. Discrete complexes may therefore be more straight-forward in terms of synthesis and application, but these catalysts require new strategies to overcome these challenges, which have not yet been developed. This section will highlight potential strategies that we believe have potential to advance this biocompatibility.

3.1. Kinetic Protection of the Catalyst

Fast reaction kinetics may be enough to allow sufficient TONs under cellular conditions. If the rate of product formation is sufficiently faster than the rate of biomolecule binding to the metal centre, then the product would be formed in good yields before the catalyst is poisoned. This may be one of the reasons that the CuAAC reaction is so successful in cells, as it is known to have very fast reaction kinetics. Reek et al. have recently demonstrated this kinetic protection for a ring-closing metathesis reaction under biological conditions in the lab, where a catalyst with faster reaction rates is able to generate higher amounts of the desired product in the presence of poisonous biomolecules compared to a similar catalyst with much slower reaction rates.[66] Although this strategy works well for this metathesis reaction, in-depth mechanistic insights may be required in order to apply this concept to other reactions.

3.2. Physical Protection of the Catalyst

Spatial separation of the metal catalyst from the surrounding cellular environment in order to prevent the biomolecules from binding to the metal centre would be a simple method to avoid biomolecule poisoning. Physical separation of the metal catalyst from the surrounding medium is a strategy that is already applied to allow organic transformations to take place in water. Amphiphilic surfactants aggregate in water to generate a micelle with a hydrophilic exterior, rendering the structure water-soluble, and a hydrophobic interior, which can house water-insoluble organic molecules.[67] Micelles have been used as a vehicle to allow a variety of different organic-soluble metal catalysed transformations to take place within the hydrophobic core of the micelle while using water as solvent.[68] Similarly, liposomes and lipid nanoparticles (LNPs) generate an interior hydrophobic cavity surrounded by a lipid bilayer, within which hydrophobic and non-cell permeable cargo can be delivered into cells.[69] Recently, lipid nanoparticle assemblies have also been shown to house catalytically active palladium nanoparticles.[70] These assemblies provide the means to both ensure the solubilisation of reaction components and their uptake into cells; however, this strategy could fall short for more polar substrates.

Alternatively, a synthetic supramolecular metallocage may also be a good host for transition metal catalysts in cells. Metallocages are typically easy to prepare, as they are formed from the self-assembly of simple metal precursors and organic building blocks that can coordinate to the metal nodes. The important properties such as the shape, size and stability can be controlled by choosing the proper building blocks, allowing for flexibility in design for the desired application. These structures are known to encapsulate both organic and metallic catalytically active species that can participate in a range of transformations.[71] Encapsulated transition metal catalysts often display different and interesting reactivity compared to free species (Figure 21). A small number of cages have demonstrated the ability to distinguish between substrates based on size.[72] This is a very promising concept for the protection of transition metal catalysts inside cells—while biomolecules that are the same size or smaller than the desired substrate would not be excluded based upon size, it is reasonable to assume that a cage would provide a means by which large or bulky catalyst poisons could be spatially separated from the catalyst. In addition, catalyst encapsulation has been shown to improve catalyst stabilisation, allowing for improved yields and TONs,[73] decreased deactivation,[74] and improved reactivity at very low catalyst loadings.[75] It is therefore possible that encapsulation of the catalyst may provide a route to faster reaction times, and therefore also bestow kinetic protection upon the reaction. The applicability of this concept to cells has already been somewhat illustrated. Recently, a supramolecular protection strategy has been shown to improve the bioorthogonality of a gold catalysed hydroarylation. While the reaction catalysed by the free gold complex was completely inhibited by the presence of biological additives, the reaction proceeded when the gold complex was encapsulated within the protective cavity of the cage, leading to formation of a fluorescent amino coumarin product, albeit in lower yields than the reaction in the absence of biological additives. The cage was shown to be impermeable to the cell membrane, so evaluation of the reaction inside cells was not possible.[76] Therefore it is still unknown if this strategy will also aid other catalysts for other reactions in cells.

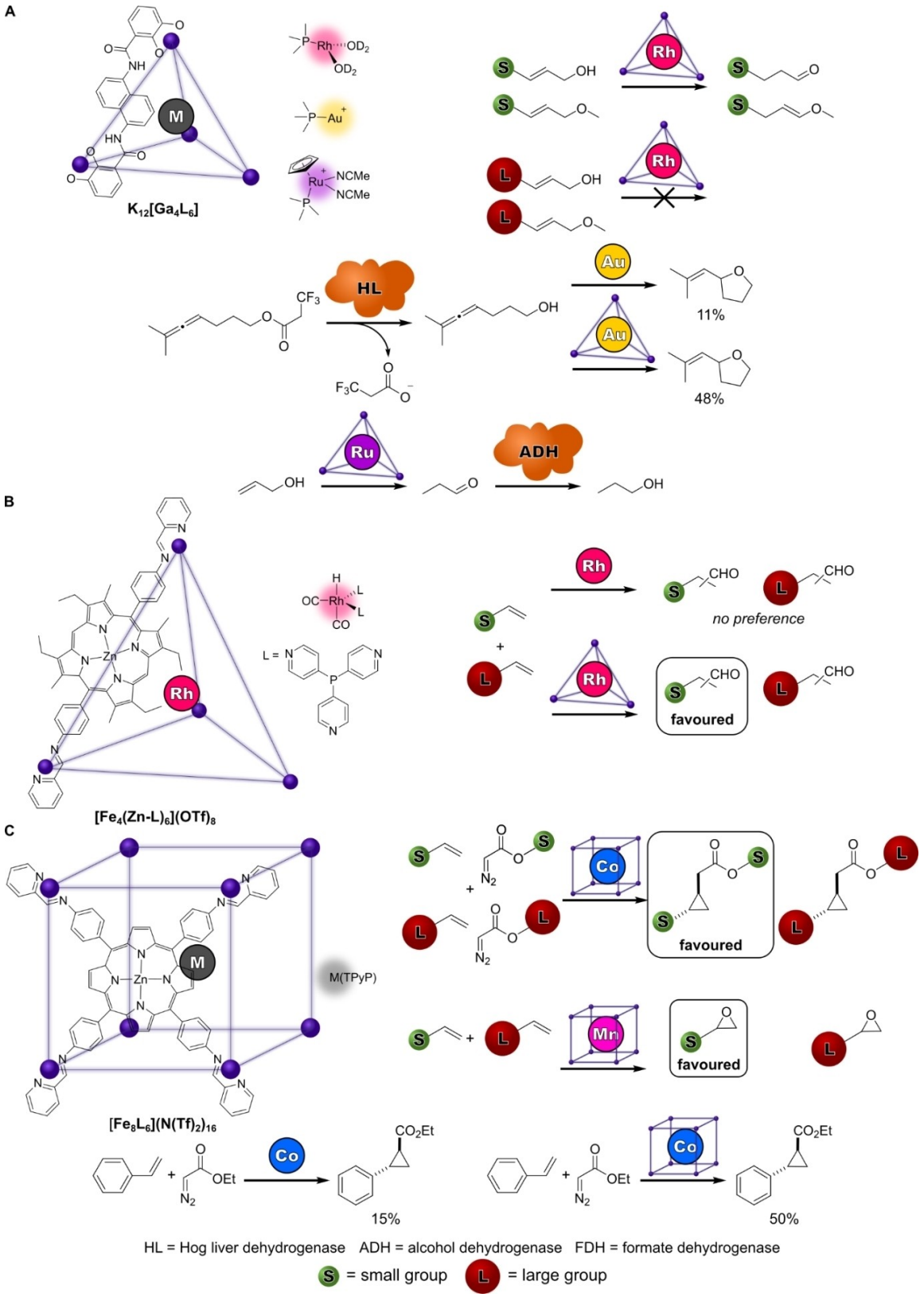

Figure 21. (a) Ga_4L_6 tetrahedral cage encapsulates small cationic catalysts for: size-selective rhodium catalysed isomerisation of allyl alcohols and ethers;[72b] tandem enzyme catalysis—gold catalysed allene hydroalkoxylation;[73a,c] and tandem ruthenium catalysed allyl alcohol isomerisation—enzyme catalysis.[73b,c] (b) Encapsulation of a rhodium complex inside the tetrahedral $Fe_4(Zn{-}L)_6$ cage imparts size selectivity upon the hydroformylation of terminal alkenes.[72c] (c) Cubic $[Fe_8L_6](N(Tf_2)_{16}$ cage encapsulates metal tetra(4-pyridyl)metalloporphyrins for: size-selective cobalt catalysed cyclopropanation of styrene and diazo substrates;[72d] size-selective manganese catalysed epoxidation of styrene substrates;[72e] and the improved yield of cobalt catalysed cyclopropanation of styrene and ethyl diazoacetate.[74b]

Although the metallocage may improve the reactivity of the metal catalyst, a pertinent question is of course its compatibility with the cellular components. As the inside of a cell is an aqueous environment, ideally the cage should be soluble and stable in aqueous solution. Many water soluble architectures have been reported, and, as previously discussed, are able to house catalytically active species. However, it is important to consider how water solubility is achieved. Typically, it can either be due to the inclusion of water soluble building blocks, or from the presence of water solubilising counterions. Clearly, for application in living cells that are full of ions, the only option is the use of building blocks that are themselves soluble in water as solubility based on counterions may result in precipitation after ion exchange.[77]

Small anions such as chlorides can have a considerable effect on cage integrity. Palladium metal centres combined with pyridyl-derived building blocks are commonly used to create a range of 3D structures.[78] Although the coordination dynamics at the palladium centre is useful for the assembly of these cages, the consequence also is the instability in the presence of chlorides. The presence of chlorides triggers decomposition of the desired cage structure due to the formation of palladium-chloride bonds.[79] Crowley et al. make use of this chloride-induced structural change to trigger cage decomposition and release cargo from the cavity.[80] A small palladium cage has been used in cells as a drug delivery system. Here, the cage itself is intended only as a vessel in which to carry cisplatin as cargo. However, no data on the stability of the cage itself under physiological conditions, or of its drug delivery mechanism, is provided.[81] The fact that palladium cages are typically not stable to chlorides calls the integrity of the cage into question once it has reached the inside of the cell, or, if it can even penetrate the cell at all. Interestingly, platinum analogues of palladium cages are a chloride-stable alternative. Platinum architectures are more stable than their palladium counterparts: while a palladium cage decomposes in the presence of acid, base, or strong nucleophile, a platinum analogue of the same cage is kinetically more inert and remains intact.[82] Indeed while the more dynamic nature of the palladium-pyridyl bonds within the palladium cages generally leads to quantitative formation of the desired structure, the stability of the platinum-pyridyl bond results in less straightforward sphere formation. High temperatures are therefore required to drive the reaction towards the most stable structure, and avoid undesired kinetic traps of smaller structures.[83] Here, chlorides can actually have a positive impact upon the cage formation, with the presence of chlorides actually aiding the formation of the desired structures from these kinetic traps, by labilising the metal-ligand bonds.[84] Therefore, it is important to consider the impact of the surrounding anions upon the metal cornerstones of the cages before selecting a structure for use in cells.

Clearly the choice of metal centre is vitally important for designing a cage that would be stable to a biological environment. In addition, ideally the cage should be inert towards the cells themselves: in order for the catalysis to actually be able to take place inside the cell, the cage itself should not be toxic, and should not influence the cellular environment or participate in its own reactions. While there are in fact a small number of examples of metal organic cages being applied in living cells, most of which are platinum based, often they are used as cytotoxic agents themselves in cancer cells.[85] In general, metal ions exhibit cytotoxicity towards cells. This is exemplified by the investigation of ruthenium, gold, platinum, palladium, silver, rhodium, copper, molybdenum, osmium, and iridium complexes as anticancer agents.[86] However, the degree of cytotoxicity that is induced by the metal complex is highly dependent upon the ligand infrastructure surrounding the metal centre, as well as the oxidation state and redox potential of the metal ion itself.[87] Therefore, it is difficult to predict the degree of cytotoxicity that will be observed for any given transition metal catalyst or metallocage. In order to circumvent toxicity problems, the IC50 value of all metal-containing compounds involved in the reaction should first be determined, and then all cell experiments conducted at metal concentrations below this value.

4. Conclusions

Although still in its infancy, the field of transition metal catalysis in living cells shows a lot of promise. This new method of in cell reactivity grants access to non-natural transformations and paves the way to achieving targeted and selective drug therapies. Many systems with different mechanisms of action have been developed that are able to kill cancer cells with high levels of efficiency, or activate anticancer prodrugs. However, there is clearly a long way to go before any such system could have a practical, real-world biomedical application. The major downfall of metal catalysts is their poor stability to the cellular environment. Facile poisoning of the catalysts results in sluggish, almost stoichiometric, reactivity. As a result high catalyst loadings are required to achieve acceptable yields. To overcome this hurdle, progress needs to be made in order to prevent catalyst deactivation and improve catalytic efficiency. Future research into spatial separation or fast reaction kinetics may be useful strategies to bring about great headway to this emerging field.

Conflict of Interest

The authors declare no conflict of interest.

Data Availability Statement

Data sharing is not applicable to this article as no new data were created or analyzed in this study.

Keywords: Biocatalysis · Bioinorganic Chemistry · Heterogeneous Catalysis · Homogeneous Catalysis · Supramolecular Chemistry

[1] a) C. J. Borths, S. D. Walker, *Isr. J. Chem.* **2020**, *60*, 340–350; b) J. E. Zweig, D. E. Kim, T. R. Newhouse, *Chem. Rev.* **2017**, *117*, 11680–11752.

[2] a) L. Hedstrom, *Enzyme Specificity and Selectivity* In *Encyclopedia of Life Sciences (ELS)*, John Wiley & Sons, Ltd, Chichester, **2010**; b) M. T. Reetz, J. D. Carballeira, J. Peyralans, H. Höbenreich, A. Maichele, A. Vogel, *Chem. Eur. J.* **2006**, *12*, 6031–6038.

[3] a) H. Madec, F. Figueiredo, K. Cariou, S. Roland, M. Sollogoub, G. Gasser, *Chem. Sci.* **2023**, *14*, 409; b) M. O. N. van de L'Isle, M. C. Ortega-Liebana, A. Unciti-Broceta, *Curr. Opin. Chem. Biol.* **2021**, *61*, 32–42; c) A. Seoane, J. L. Mascareñas, *Eur. J. Org. Chem.* **2022**, e202200118; d) P. Destito, C. Vidal, F. López, J. L. Mascareñas, *Chem. Eur. J.* **2021**, *27*, 4789; e) W. Wang, X. Zhang, R. Huang, C.-M. Hirschbiegel, H. Wang, Y. Ding, V. M. Rotello *Adv. Drug Delivery Rev.* **2021**, *176*, 113893.

[4] V. S. Dave, D. Gupta, M. Yu, P. Nguyen, S. Varghese Gupta, *Drug Dev. Ind. Pharm.* **2017**, *43*, 177–189.

[5] H. J. Forman, H. Zhang, A. Rinna, *Mol. Aspects Med.* **2009**, *30*, 1–12.

[6] K. Le Gal, E. E. Schmidt, V. I. Sayin, *Antioxidants* **2021**, *10*, 1377.

[7] S. J. Dougan, A. Habtemariam, S. E. McHale, S. Parsons, P. J. Sadler, *Proc. Natl. Acad. Sci. USA* **2008**, *105*, 11628.

[8] A. Meister, M. E. Anderson, *Annu. Rev. Biochem.* **1983**, *52*, 711–760.

[9] H. Y. Huang, S. Banerjee, K. Qiu, P. Zhang, O. Blacque, T. Malcomson, M. J. Paterson, G. J. Clarkson, M. Staniforth, V. G. Stavros, G. Gasser, H. Chao, P. J. Sadler, *Nat. Chem.* **2019**, *11*, 1041.

[10] D. Nolfi-Donegan, A. Braganza, S. Shiva, *Redox Biol.* **2020**, *37*, 101674.

[11] P. K. Sasmal, S. Carregal-Romero, A. A. Han, C. N. Streu, Z. Lin, K. Namikawa, S. L. Elliott, R. W. Köster, W. J. Parak, E. Meggers, *ChemBioChem* **2012**, *13*, 1116–1120.

[12] K. K. Sadhu, T. Eierhoff, W. Römer, N. Winssinger, *J. Am. Chem. Soc.* **2012**, *134*, 20013–20016.

[13] K. K. Sadhu, E. Lindberg, N. Winssinger, *Chem. Commun.* **2015**, *51*, 16664–16666.

[14] K. K. Sadhu, N. Winssinger, *Chem. Eur. J.* **2013**, *19*, 8182–8189.

[15] L. Holtzer, I. Oleinich, M. Anzola, E. Lindberg, K. K. Sadhu, M. Gonzalez-Gaitan, N. Winssinger, *ACS Cent. Sci.* **2016**, *2*, 394–400.

[16] J. Chen, K. Li, J. S. L. Shon, S. C. Zimmerman, *J. Am. Chem. Soc.* **2020**, *142*, 4565–4569.

[17] S. Bose, A. H. Ngo, L. H. Do, *J. Am. Chem. Soc.* **2017**, *139*, 8792–8795.

[18] Z. Liu, I. Romero-Canelón, B. Qamar, J. M. Hearn, A. Habtemariam, N. P. E. Barry, A. M. Pizarro, G. J. Clarkson, P. J. Sadler, *Angew. Chem. Int. Ed.* **2014**, *53*, 3941–3946.

[19] L. Yang, S. Bose, A. H. Ngo, L. H. Do, *ChemMedChem* **2017**, *12*, 292–299.

[20] J. J. Soldevila-Barreda, I. Romero-Canelón, A. Habtemariam, P. J. Sadler, *Nat. Commun.* **2015**, *6*, 6582.

[21] J. J. Soldevila-Barreda, A. Habtemariam, I. Romero-Canelón, P. J. Sadler, *J. Inorg. Biochem.* **2015**, *153*, 322–333.

[22] J. P. C. Coverdale, I. Romero-Canelón, C. Sanchez-Cano, G. J. Clarkson, A. Habtemariam, M. Wills, P. J. Sadler, *Nat. Chem.* **2018**, *10*, 347–354.

[23] E. M. Bolitho, J. P. C. Coverdale, H. E. Bridgewater, G. J. Clarkson, P. D. Quinn, C. Sanchez-Cano, P. J. Sadler, *Angew. Chem. Int. Ed.* **2021**, *60*, 6462–6472.

[24] C. Vidal, M. Tomas-Gamasa, A. Gutierrez-Gonzalez, J. L. Mascareñas, *J. Am. Chem. Soc.* **2019**, *141*, 5125–5129.

[25] C. Streu, E. Meggers, *Angew. Chem. Int. Ed.* **2006**, *45*, 5645–5648.

[26] M. I. Sanchez, C. Penas, M. E. Vazquez, J. L. Mascareñas, *Chem. Sci.* **2014**, *5*, 1901–1907.

[27] R. Das, R. F. Landis, G. Y. Tonga, R. Cao-Milán, D. C. Luther, V. M. Rotello, *ACS Nano* **2019**, *13*, 229–235.

[28] P. K. Sasmal, S. Carregal-Romero, W. J. Parak, E. Meggers, *Organometallics* **2012**, *31*, 5968–5970.

[29] T. Völker, F. Dempwolff, P. L. Graumann, E. Meggers, *Angew. Chem. Int. Ed.* **2014**, *53*, 10536–10540.

[30] T. Volker, E. Meggers, *ChemBioChem* **2017**, *18*, 1083–1086.

[31] M. Tomás-Gamasa, M. Martínez-Calvo, J. R. Couceiro, J. L. Mascareñas, *Nat. Commun.* **2016**, *7*, 12538.

[32] J. DeChancie, K. N. Houk, *J. Am. Chem. Soc.* **2007**, *129*, 5419–5429.

[33] F. Liu, J. Z. H. Zhang, Y. Mei, *Sci. Rep.* **2016**, *6*, 27190.

[34] Y. Okamoto, R. Kojima, F. Schwizer, E. Bartolami, T. Heinisch, S. Matile, M. Fussenegger, T. R. Ward, *Nat. Commun.* **2018**, *9*, 7.

[35] M. Santra, S.-K. Ko, I. Shin, K. H. Ahn, *Chem. Commun.* **2010**, *46*, 3964–3966.

[36] M. Martínez-Calvo, J. R. Couceiro, P. Destito, J. Rodríguez, J. Mosquera, J. L. Mascareñas, *ACS Catal.* **2018**, *8*, 6055–6061.

[37] G. Y. Tonga, Y. Jeong, B. Duncan, T. Mizuhara, R. Mout, R. Das, S. T. Kim, Y.-C. Yeh, B. Yan, S. Hou, V. M. Rotello, *Nat. Chem.* **2015**, *7*, 597–603.

[38] T. Lv, J. Wu, F. Kang, T. Wang, B. Wan, J.-J. Lu, Y. Zhang, Z. Huang, *Org. Lett.* **2018**, *20*, 2164–2167.

[39] T. Sun, T. Lv, J. Wu, M. Zhu, Y. Fei, J. Zhu, Y. Zhang, Z. Huang, *J. Med. Chem.* **2020**, *63*, 13899–13912.

[40] E. Indrigo, J. Clavadetscher, S. V. Chankeshwara, A. Megia-Fernandez, A. Lilienkampfa, M. Bradley, *Chem. Commun.* **2017**, *53*, 6712–6715.

[41] S. Learte-Aymamí, C. Vidal, A. Gutiérrez-González, J. L. Mascareñas, *Angew. Chem. Int. Ed.* **2020**, *59*, 9149–9154.

[42] J. Wang, S. Zheng, Y. Liu, Z. Zhang, Z. Lin, J. Li, G. Zhang, X. Wang, J. Li, P. R. Chen, *J. Am. Chem. Soc.* **2016**, *138*, 15118–15121.

[43] X. Wang, Y. Liu, X. Fan, J. Wang, W. S. C. Ngai, H. Zhang, J. Li, G. Zhang, J. Lin, P. R. Chen, *J. Am. Chem. Soc.* **2019**, *141*, 17133–17141.

[44] C. Vidal, M. Tomás-Gamasa, P. Destito, F. López, J. L. Mascareñas, *Nat. Commun.* **2018**, *9*, 1913.

[45] Y. Long, B. Cao, X. Xiong, A. S. C. Chan, R. W.-Y. Sun, T. Zou, *Angew. Chem. Int. Ed.* **2021**, *60*, 4133–4141.

[46] K. Vong, T. Yamamoto, T.-C. Chang, K. Tanaka, *Chem. Sci.* **2020**, *11*, 10928–10933.

[47] T.-C. Chang, K. Vong, T. Yamamoto, K. Tanaka, *Angew. Chem.* **2021**, *133*, 12554–12562.

[48] B. L. Oliveira, B. J. Stenton, V. B. Unnikrishnan, C. R. de Almeida, J. Conde, M. Negrão, F. S. S. Schneider, C. Cordeiro, M. G. Ferreira, G. F. Caramori, J. B. Domingos, R. Fior, G. J. L. Bernardes, *J. Am. Chem. Soc.* **2020**, *142*, 10869–10880.

[49] a) M. Yu, S. Lou, F. Gonzalez-Bobes, *Org. Process Res. Dev.* **2018**, *22*, 918–946; b) C. S. Higman, J. A. M. Lummiss, D. E. Fogg, *Angew. Chem. Int. Ed.* **2016**, *55*, 3552–3565.

[50] a) M. S. Messina, H. D. Maynard, *Mater. Chem. Front.* **2020**, *4*, 1040–1051; b) Y. A. Lin, J. M. Chalker, B. G. Davis, *ChemBioChem* **2009**, *10*, 959–969; c) Y. A. Lin, O. Boutureira, L. Lercher, B. Bhushan, R. S. Paton, B. G. Davis, *J. Am. Chem. Soc.* **2013**, *135*, 12156–12159; d) J. M. Chalker, Y. A. Lin, O.

Boutureira, B. G. Davis, *Chem. Commun.* **2009**, 3714–3716; e) A. Brik, *Adv. Synth. Catal.* **2008**, *350*, 1661–1675.
[51] S. Eda, I. Nasibullin, K. Vong, N. Kudo, M. Yoshida, A. Kurbangalieva, K. Tanaka, *Nat. Catal.* **2019**, *2*, 780–792.
[52] S. Li, L. Wang, F. Yu, Z. Zhu, D. Shobaki, H. Chen, M. Wang, J. Wang, G. Qin, U. J. Erasquin, L. Ren, Y. Wang, C. Cai, *Chem. Sci.* **2017**, *8*, 2107–2114.
[53] J. Miguel-Avila, M. Tomas-Gamasa, A. Olmos, P. J. Perez, J. L. Mascareñas, *Chem. Sci.* **2018**, *9*, 1947–1952.
[54] P. Destito, J. R. Couceiro, H. Faustino, F. López, J. L. Mascareñas, *Angew. Chem. Int. Ed.* **2017**, *56*, 10766–10770.
[55] A. Gutiérrez-González, P. Destito, J. R. Couceiro, C. Pérez-González, F. López, J. L. Mascareñas, *Angew. Chem. Int. Ed.* **2021**, *60*, 16059.
[56] J. Miguel-Ávila, M. Tomás-Gamasa, J. L. Mascareñas, *Angew. Chem. Int. Ed.* **2020**, *59*, 17628.
[57] W. Song, N. Zheng, *Org. Lett.* **2017**, *19*, 6200–6203.
[58] R. Chen, L. Zeng, Z. Lai, S. Cui, *Adv. Synth. Catal.* **2019**, *361*, 989–994.
[59] M. Li, N. Zheng, J. Li, Y. Zheng, W. Song, *Green Chem.* **2020**, *22*, 2394–2398.
[60] R. Chinchilla, C. Nájera, *Chem. Soc. Rev.* **2011**, *40*, 5084–5121.
[61] a) N. Li, R. K. V. Lim, S. Edwardraja, Q. Lin, *J. Am. Chem. Soc.* **2011**, *133*, 15316–15319; b) N. Li, C. P. Ramil, R. K. V. Lim, Q. Lin, *ACS Chem. Biol.* **2015**, *10*, 379–384; c) J. Li, S. Lin, J. Wang, S. Jia, M. Yang, Z. Hao, X. Zhang, P. R. Chen, *J. Am. Chem. Soc.* **2013**, *135*, 7330–7338.
[62] R. M. Yusop, A. Unciti-Broceta, E. M. V. Johansson, R. M. Sánchez-Martín, M. Bradley, *Nat. Chem.* **2011**, *3*, 239–243.
[63] a) F. Wang, Y. Zhang, Z. Du, J. Ren, X. Qu, *Nat. Commun.* **2018**, *9*, 1209; b) J. Clavadetscher, E. Indrigo, S. V. Chankeshwara, A. Lilienkampf, M. Bradley, *Angew. Chem. Int. Ed.* **2017**, *56*, 6864–6868.
[64] K. Tsubokura, K. K. H. Vong, A. R. Pradipta, A. Ogura, S. Urano, T. Tahara, S. Nozaki, H. Onoe, Y. Nakao, R. Sibgatullina, A. Kurbangalieva, Y. Watanabe, K. Tanaka, *Angew. Chem. Int. Ed.* **2017**, *56*, 3579–3584.
[65] C. E. Valdez, Q. A. Smith, M. R. Nechay, A. N. Alexandrova, *Acc. Chem. Res.* **2014**, *47*, 3110–3117.
[66] C. C. James, P. C. M. Laan, B. De Bruin, J. N. H. Reek, *ChemCatChem*, **2023**, *15*, e202201272.
[67] M. P. Andersson, F. Gallou, P. Klumphu, B. S. Takale, B. H. Lipshutz, *Chem. Eur. J.* **2018**, *24*, 6778–6786.
[68] a) M. Cortes-Clerget, N. Akporji, J. Zhou, F. Gao, P. Guo, M. Parmentier, F. Gallou, J.-Y. Berthon, B. H. Lipshutz, *Nat. Commun.* **2019**, *10*, 2169; b) B. H. Lipshutz, S. Ghorai, A. R. Abela, R. Moser, T. Nishikata, C. Duplais, A. Krasovskiy, R. D. Gaston, R. C. Gadwood, *J. Org. Chem.* **2011**, *76*, 4379–4391; c) B. Lipshutz, *Curr. Opin. Green Sustain. Chem.* **2018**, *11*, 1–8; d) S. Wallace, E. Balskus, *Angew. Chem. Int. Ed.* **2016**, *55*, 6023–6027.
[69] a) F. Campbell, F. L. Bos, S. Sieber, G. Arias-Alpizar, B. E. Koch, J. Huwyler, A. Kros, J. Bussmann, *ACS Nano* **2018**, *12*, 2138–2150; b) Y. Hayashi, M. Takamiya, P. B. Jensen, I. Ojea-Jiménez, H. Claude, C. Antony, K. Kjaer-Sorensen, C. Grabher, T. Boesen, D. Gilliland, *ACS Nano* **2020**, *14*, 1665–1681; c) G. Arias-Alpizar, L. Kong, R. C. Vlieg, A. Rabe, P. Papadopoulou, M. S. Meijer, S. Bonnet, S. Vogel, J. van Noort, A. Kros, *Nat. Commun.* **2020**, *11*, 3638; d) L. van der Koog, T. B. Gandek, A. Nagelkerke, *Adv. Healthcare Mater.* **2022**, *11*, 2100639.
[70] D. D. Ortega, N. Pavlakovich, Y.-S. Shon, *RSC Adv.* **2022**, *12*, 21866.
[71] Y. Fang, J. A. Powell, E. Li, Q. Wang, Z. Perry, A. Kirchon, X. Yang, Z. Xiao, C. Zhu, L. Zhang, F. Huang, H.-C. Zhou, *Chem. Soc. Rev.* **2019**, *48*, 4707–4730.
[72] a) D. H. Leung, R. G. Bergman, K. N. Raymond, *J. Am. Chem. Soc.* **2006**, *128*, 9781–9797; b) D. H. Leung, R. G. Bergman, K. N. Raymond, *J. Am. Chem. Soc.* **2007**, *129*, 2746–2747; c) S. S. Nurttila, W. Brenner, J. Mosquera, K. M. van Vliet, J. R. Nitschke, J. N. H. Reek, *Chem. Eur. J.* **2019**, *25*, 609–620; d) M. Otte, P. F. Kuijpers, O. Troeppner, I. Ivanović-Burmazović, J. N. H. Reek, B. de Bruin, *Chem. Eur. J.* **2014**, *20*, 4880–4884; e) P. F. Kuijpers, M. Otte, M. Dürr, I. Ivanović-Burmazović, J. N. H. Reek, B. de Bruin, *ACS Catal.* **2016**, *6*, 3106–3112.
[73] a) Z. J. Wang, C. J. Brown, R. G. Bergman, K. N. Raymond, F. D. Toste, *J. Am. Chem. Soc.* **2011**, *133*, 7358–7360; b) C. J. Brown, G. M. Miller, M. W. Johnson, R. G. Bergman, K. N. Raymond, *J. Am. Chem. Soc.* **2011**, *133*, 11964–11966; c) Z. J. Wang, K. N. Clary, R. G. Bergman, K. N. Raymond, F. D. Toste, *Nat. Chem.* **2013**, *5*, 100–103.
[74] a) D. M. Kaphan, M. D. Levin, R. G. Bergman, K. N. Raymond, F. D. Toste, *Science* **2015**, *350*, 1235; b) M. Otte, P. F. Kuijpers, O. Troeppner, I. Ivanović-Burmazović, J. N. H. Reek, B. de Bruin, *Chem. Eur. J.* **2013**, *19*, 10170–10178; c) L. J. Jongkind, M. Rahimi, D. Poole Iii, S. J. Ton, D. E. Fogg, J. N. H. Reek, *ChemCatChem* **2020**, *12*, 4019–4023.
[75] a) C. Tan, J. Jiao, Z. Li, Y. Liu, X. Han, Y. Cui, *Angew. Chem. Int. Ed.* **2018**, *57*, 2085–2090; b) J. Jiao, C. Tan, Z. Li, Y. Liu, X. Han, Y. Cui, *J. Am. Chem. Soc.* **2018**, *140*, 2251–2259.
[76] C. C. James, D. Wu, E. O. Bobylev, A. Kros, B. de Bruin, J. N. H. Reek, *ChemCatChem* **2022**, *14*, e202200942.
[77] E. G. Percástegui, J. Mosquera, T. K. Ronson, A. J. Plajer, M. Kieffer, J. R. Nitschke, *Chem. Sci.* **2019**, *10*, 2006–2018.
[78] D. Bardhan, D. K. Chand, *Chem. Eur. J.* **2019**, *25*, 12241–12269.
[79] E. O. Bobylev, B. de Bruin, J. N. H. Reek, *Inorg. Chem.* **2021**, *60*, 12498–12505.
[80] D. Preston, A. Fox-Charles, W. K. C. Lo, J. D. Crowley, *Chem. Commun.* **2015**, *51*, 9042–9045.
[81] J. Han, A. F. B. Räder, F. Reichart, B. Aikman, M. N. Wenzel, B. Woods, M. Weinmüller, B. S. Ludwig, S. Stürup, G. M. M. Groothuis, H. P. Permentier, R. Bischoff, H. Kessler, P. Horvatovich, A. Casini, *Bioconjugate Chem.* **2018**, *29*, 3856–3865.
[82] F. Ibukuro, T. Kusukawa, M. Fujita, *J. Am. Chem. Soc.* **1998**, *120*, 8561–8562.
[83] E. O. Bobylev, D. A. Poole III, B. de Bruin, J. N. H. Reek, *Chem. Sci.* **2021**, *12*, 7696–7705.
[84] E. O. Bobylev, D. A. Poole III, B. de Bruin, J. N. H. Reek, *Chem. Eur. J.* **2021**, *27*, 12667–12674.
[85] a) A. Ahmedova, *Front. Chem.* **2018**, *6*, 20; b) H. Sepehrpour, W. X. Fu, Y. Sun, P. J. Stang, *J. Am. Chem. Soc.* **2019**, *141*, 14005–14020.
[86] U. Ndagi, N. Mhlongo, M. E. Soliman, *Drug Des. Dev. Ther.* **2017**, *11*, 599–616.
[87] D. A. Guk, O. O. Krasnovskaya, E. K. Beloglazkina, *Russ. Chem. Rev.* **2021**, *90*, 1566–1623.

Manuscript received: May 12, 2023
Accepted manuscript online: June 20, 2023
Version of record online: July 7, 2023